Differentiation 133 (2023) 25–39

Contents lists available at ScienceDirect

Differentiation

journal homepage: www.elsevier.com/locate/diff

Ex vivo adult stem cell characterization from multiple muscles in ambulatory children with cerebral palsy during early development of contractures

M. Corvelyn [a], J. Meirlevede [a], J. Deschrevel [b], E. Huyghe [c], E. De Wachter [d], G. Gayan-Ramirez [b], M. Sampaolesi [a], A. Van Campenhout [d,e], K. Desloovere [c,**,1], D. Costamagna [a,c,*,1]

[a] Stem Cell and Developmental Biology, Dept. of Development and Regeneration, KU Leuven, Belgium
[b] Laboratory of Respiratory Diseases and Thoracic Surgery, Dept. of Chronic Diseases and Metabolism, KU Leuven, Belgium
[c] Research Group for Neurorehabilitation, Dept. of Rehabilitation Sciences, KU Leuven, Belgium
[d] Dept. of Orthopaedic Surgery, University Hospitals Leuven, Belgium
[e] Dept. of Development and Regeneration, KU Leuven, Belgium

ARTICLE INFO

Keywords:
Muscle stem cells
Cerebral palsy
Young patients
Myogenesis
Lower limb muscle comparisons
Medial gastrocnemius
Semitendinosus

ABSTRACT

Cerebral palsy (CP) is one of the most common conditions leading to lifelong childhood physical disability. Literature reported previously altered muscle properties such as lower number of satellite cells (SCs), with altered fusion capacity. However, these observations highly vary among studies, possibly due to heterogeneity in patient population, lack of appropriate control data, methodology and different assessed muscle.

In this study we aimed to strengthen previous observations and to understand the heterogeneity of CP muscle pathology. Myogenic differentiation of SCs from the *Medial Gastrocnemius* (MG) muscle of patients with CP (n = 16, 3–9 years old) showed higher fusion capacity compared to age-matched typically developing children (TD, n = 13). Furthermore, we uniquely assessed cells of two different lower limb muscles and showed a decreased myogenic potency in cells from the *Semitendinosus* (ST) compared to the MG (TD: n = 3, CP: n = 6). Longitudinal assessments, one year after the first botulinum toxin treatment, showed slightly reduced SC representations and lower fusion capacity (n = 4). Finally, we proved the robustness of our data, by assessing in parallel the myogenic capacity of two samples from the same TD muscle.

In conclusion, these data confirmed previous findings of increased SC fusion capacity from MG muscle of young patients with CP compared to age-matched TD. Further elaboration is reported on potential factors contributing to heterogeneity, such as assessed muscle, CP progression and reliability of primary outcome parameters.

1. Introduction

With an incidence of 1 in 500 live births, cerebral palsy (CP) is one of the most common conditions leading to lifelong childhood physical disability (Oskoui et al., 2013). It is considered to be originated from a neural lesion in the immature brain, leading to progressive musculoskeletal symptoms. Clinically, CP manifests itself on both neural and muscular level (spasticity, increased muscle stiffness and contractures, decreased strength and muscular control), resulting in decreased functional ability such as disturbed gait (Howard et al., 2022; Mathewson and Lieber, 2015; Romero et al., 2021). These patients can be classified following the Gross Motor Function Classification System (GMFCS), from levels I to V, based on their functional abilities and limitations (R. Palisano et al., 2008; R.J. Palisano et al., 2008). Treatment mainly consists of management of the symptoms at the muscle level, including physiotherapy, orthoses, Botulinum Neurotoxin A (BoNT) injections and orthopaedic surgery (Howard et al., 2022; Novak, 2014). However, knowledge on the effects of treatment on CP muscle morphology is incomplete and totally lacking on cellular level (Howard et al., 2022). Hence, there is much interest in better understanding the underlying

* Corresponding author. University Hospital Gasthuisberg Herestraat, 49, O&N4-BUS, 814, 3000, Leuven, Belgium.
** Corresponding author. University Hospital Pellenberg, UZ Leuven, Weligerveld 1, 3212, Pellenberg, Belgium.
E-mail addresses: kaat.desloovere@kuleuven.be (K. Desloovere), domiziana.costamagna@kuleuven.be (D. Costamagna).
[1] These authors share last authorship.

https://doi.org/10.1016/j.diff.2023.06.003
Received 23 November 2022; Received in revised form 25 May 2023; Accepted 27 June 2023
Available online 12 July 2023

pathomorphology of skeletal muscles in patients with CP and thereby as well the effects of treatment (Romero et al., 2021).

Literature has reported altered muscle properties compared to typically developing (TD) muscles, mainly in adolescents and adults. Microscopically, increased collagen content and abnormal organization in the extra-cellular matrix have been reported and linked to muscle stiffness (Pingel et al., 2021; Smith et al., 2019). Furthermore, some studies have reported smaller muscle fibers, varying predominance of muscle fiber type and higher intramuscular fat fractions (Booth et al., 2001; Johnson et al., 2009; Marbini et al., 2002; Smith et al., 2011). On cellular level, some groups have already shown a significant reduction in numbers of satellite cells (SCs) in contractured muscle of patients with CP (Dayanidhi et al., 2015; Smith et al., 2013; Von Walden et al., 2018), the primary source of stem cells involved in muscle growth and regeneration processes postnatally by fusion with damaged muscle fibers. To this end, studies in mouse models previously showed that prepubertal SC depletion resulted in lifelong deficits in muscle mass and regenerative capacity, with lower myogenic commitment of the remaining SCs (Bachman et al., 2020; Murach et al., 2017). However, research on the functionality of these SCs in the muscles of patients with CP is scarce. Domenighetti et al. described lower fusion index (FI) values in CP-derived SC-derived myoblasts (patients aged 3–18 years, average age of 9 years) and smaller myotubes compared to those of TD adolescents (aged 14–18 years, average age of 15 years), based on hamstring biopsies (Domenighetti et al., 2018; Sibley et al., 2021). Additionally, the same group also showed that CP-derived myoblasts are hyperproliferative and this phenotype is associated with DNA hypermethylation (Sibley et al., 2021). Our group previously reported higher FI values and larger myotubes based on MyHC + areas of SC-derived myoblasts from microbiopsies of the *Medial Gastrocnemius* (MG) of younger patients with CP (aged 3–9 years) compared to aged-matched TD children (Corvelyn et al., 2020). Potential reasons for these conflicting results, such as differences in isolation material and protocol, patient diversity and the variety of the assessed muscle, have already been suggested and need to be further explored to improve the understanding of the heterogeneity of the CP muscle pathology, before drawing generalized conclusions on muscle stem cell alterations in CP (Corvelyn et al., 2020). Therefore, to shed a light on these controversies and to broaden our previous findings, we corroborated our TD sample size and better characterized the purity and myogenic potential from microbiopsy-derived SCs (Corvelyn et al., 2020). Furthermore, as the muscle-specificity could potentially partly explain the observed heterogeneity in the fusion potential of SCs, a logic next step was to isolate and characterize stem cells from different lower limb muscles, i.e. from the *Medial Gastrocnemius* (MG) and *Semitendinosus* (ST). Lastly, more knowledge on the reliability of stem cell characterization parameters based on repeated assessments could further strengthen the value of the study results. These novel data can improve the understanding of the complex nature of intrinsic muscle impairment in CP, which may eventually help to optimize treatment.

Finally, while first attempts in characterizing stem cell features of patients have been made, information on the progression of these features and on their role in treatment is still not available. Since previous studies mainly applied invasive muscle biopsy methods, no longitudinal assessments have been possible. Yet, these longitudinal data are clinically relevant. For example, muscle imaging and animal studies highlighted that BoNT injections that are planned to reduce spasticity may induce atrophy and increase the fibro/fatty content in the muscle (Howard et al., 2022; Sätilä, 2020; Walhain et al., 2021). Though, the effects of BoNT on microscopical level or on the stem cells of the muscle are much less studied, but are required for optimizing treatment.

In addition to SCs, also mesoangioblasts (MABs) have been recognized for their role in regeneration. Next to SCs, MABs are also able to directly fuse with damaged muscle fibers. In case of muscular dystrophies, MABs have shown to reconstitute the SC pool in case SCs were exhausted or insufficient for muscle regeneration (Dellavalle et al., 2011; Sampaolesi et al., 2006; Tedesco et al., 2017). Furthermore, also fibro-adipogenic progenitor cells (FAPs) have shown to be involved in the muscle regeneration processes, firstly by synthesizing the transient connective tissue necessary to maintain the structural integrity during regeneration and secondly by supporting myogenesis/the myogenic process by stimulating SC activation (Collins and Kardon, 2021; Joe et al., 2010; Uezumi et al., 2010). However, in cases of chronic injury, these cells start to highly proliferate and could differentiate towards adipocytes leading to adipogenic muscle loss (Hogarth et al., 2019; Uezumi et al., 2010). Unfortunately, data on the role of these progenitor cells in the light of CP muscle pathology are almost completely lacking and did not show altered differentiation capacity in young children with CP (Corvelyn et al., 2020).

Driven by the increasing indications of stem cell involvement in the altered muscle features of patients with CP (Corvelyn et al., 2020; Domenighetti et al., 2018; Sibley et al., 2021), the current study addressed a series of uncertainties that may help to understand the heterogeneity in CP muscle pathology, especially with respect to muscle stem cell behaviour. Thereby we defined three objectives for this study: confirming previous reported CP SC features by increasing TD sample size, assessing SC differences between muscles or over time and investigating multiple potential involved stem cell populations. The first objective was to analyze an increased dataset of muscle microbiopsies from age-matched TD subjects to confirm and generalize our earlier preliminary findings on SC-derived progenitors' behaviour (Corvelyn et al., 2020). Thereby, a more thorough characterization of the obtained stem cells was presented to specifically address the recent concerns indicated by Lieber and colleagues (Lieber and Domenighetti, 2021). The second objective was to investigate potential factors leading to heterogeneity of muscle stem cell features. Thereby, SC-derived myoblasts (SCMs) were collected and assessed from both the MG as well as the ST muscles of the same patients, to better understand the muscle-specificity of the observed phenotype. Additionally, using the muscle microbiopsy technique, a unique longitudinal preliminary assessment of CP-derived stem cell properties of the same muscle was performed. This allowed first insights into the natural pathway in the clinical picture of CP pathology on the level of the muscle stem cells and into the exploration of possible effects caused by previous BoNT treatment. Furthermore, for a better understanding of these longitudinal data and understanding the robustness of the primary outcome parameters, repeatability experiments were performed to quantify and decrease the risk of misinterpretation of potential effects due to the procedure or to the biopsy quality. The third objective was to examine the role of MABs, FAPs and interstitial cells (ICs) in the observed muscle alterations in both the MG and ST, cross-sectionally as well as longitudinally, i.e. prior to- and post-BoNT treatment.

2. Materials and methods

2.1. Muscle microbiopsy collection

This study protocol was approved by the Ethical Committee of the University Hospitals of Leuven, Belgium (S61110 and S62645). Written informed consent was provided by the parents. Children with cerebral palsy (CP) were recruited from the CP Reference Centre, whereas typically developing (TD) children were recruited from the Traumatology Unit for upper limb surgeries, or from the Ear, Nose and Throat Unit for other procedures at the University Hospitals Leuven (Belgium). A group of 16 patients with CP (age 3–9 years; Gross Motor Function Classification System levels I-III) and 13 age-matched TD children were included in this study. The demographics, patient characteristics and anthropometric data (age, weight and height, topographic classification, gender, GMFCS-level and treatment history) are summarized in Table 1. All children had spasticity in the *Gastrocnemius* (with modified Ashworth scores ranging from 1+ to 3) and in the hamstrings (with Modified Ashworth scores ranging from 1+ to 2). Joint mobility at the ankle and

Table 1
Demographic and anthropometric data for recruited subjects.

	CP (MG + ST analyzed)	CP (only MG analyzed)	TD (MG + ST analyzed)	TD (only MG analyzed)
Baseline				
Number of included subjects	6	10	3	10
Age in years	5.82 (1.86)	6.32 (3.16)	5.94 (1.05)	4.83 (1.46)
Weight in kg	20.75 (3.00)	19.20 (5.70)	21.00 (1.50)	18.90 (5.61)
Length in cm	116.50 (17.75)	112.00 (22.50)	116.00 (3.50)	110.00 (16.05)
Gender	Female: n = 2 Male: n = 4	Female: n = 3 Male: n = 7	Female: n = 1 Male: n = 2	Female: n = 4 Male: n = 6
Topographic involvement	CP BL: n = 5 CP UL: n = 1	CP BL: n = 0 CP UL: n = 10	NA	NA
GMFCS level: I/II/III	n = 0/5/1	n = 5/2/3	NA	NA
BoNT treatment history	0: n = 3 1-2: n = 1 3-6: n = 1 >6: n = 1	0: n = 3 1-2: n = 4 3-6: n = 3 >6: n = 0	NA	NA
One year post BoNT				
Number of included subjects	3	1		
Age in years	7.13 (0.95)	5.22 (0.00)	NA	NA
Weight in kg	21.70 (2.50)	17.70 (0.00)		
Length in cm	122.80 (10.50)	108.70 (0.00)		
Gender	Female: n = 1 Male: n = 2	Female: n = 1 Male: n = 0		
Topographic involvement	CP BL: n = 2 CP UL: n = 1	CP BL: n = 0 CP UL: n = 1		
GMFCS level: I/II/III	n = 0/3/0	n = 1/0/0		
BoNT treatment history	0: n = 0 1-2: n = 3 3-6: n = 0 >6: n = 0	0: n = 0 1-2: n = 1 3-6: n = 0 >6: n = 0		

Age, weight and length are presented as median (interquartile range). The other data are presented as frequencies. *CP: cerebral palsy, TD: typically developing, BoNT: Botulinum Neurotoxin A, n: number, GMFCS: Gross motor function classification system, BL: bilateral, UL: unilateral, MG: Medial Gastrocnemius, ST: Semitendinosus, kg=kilogram, cm=centimetre, NA: not applicable.*

knee was evaluated using goniometry. Mild to moderate fixed *Gastrocnemius* contractures were observed in 50% of the children (maximum dorsiflexion ranging between −10° and 5°), while 50% of the children had no fixed gastrocnemius contractures (maximum dorsiflexion ranging between 10° and 15°). The Modified Tardieu ankle for the gastrocnemius ranged between −30° and 0° dorsiflexion, indicating that all children had dynamic muscle contractures in the *Gastrocnemius*. Fixed contractures in the hamstrings were observed in all children, with a popliteal angle (evaluated with a neutral pelvis position) ranging between −4° and −70°. In the CP group, children with presence of dystonia or ataxia, BoNT injections within the last 6 months, orthopaedic surgery less than 2 years before data collection, as well as any previous muscle surgery on the MG or ST were excluded. Additionally, TD children were further excluded when they had a history of neurological problems or when they were involved in a high-performance sporting program (i.e. >3 h of sports activities per week). All biopsies were collected during interventions requiring general anaesthesia related to orthopaedic interventions (including BoNT-injections). Combined microbiopsies from the muscle mid-belly of the MG and of the ST in the same child were obtained for a subgroup of 6 CP and 3 TD children. Four of the enrolled children with CP were included for longitudinal assessment, for that purpose a first biopsy of the MG was taken when they were BoNT-naïve at the time of study enrolment, and a second one was collected over one year later (13–19 months after first BoNT treatment). Unfortunately, sample size for these longitudinal studies was small as the recruitment was hampered due to the COVID-19- pandemic. Two muscle biopsies for parallel stem cell assessments were obtained at the same time from the MG muscle of two TD children for the repeatability investigation of the primary outcome parameters. The biopsy collections were performed percutaneously under ultrasound guidance, with a microbiopsy needle (16-gauge, Bard). Clinical tolerance was good (based on questionnaire data obtained from parents two days post-biopsy). Furthermore, a questionnaire about the hobbies and intensity levels of activity was used for all enrolled subjects. Even though the primary goal of this study was to investigate muscle stem cell features for which the collected biopsies were entirely used, for a limited number of the enrolled patients, we could collect additional microbiopsies during the same session. These allowed explorative histological assessment of the muscle tissue via Haematoxylin and Eosin staining, as well as prospective *ex vivo* SC counting, to further describe the muscle and complement the *in vitro* cell culture data for a small subset of the participants.

2.2. Study design

For each of the three study objectives, specific analyses were planned on specific muscle samples of the entire study group or on a subgroup of the enrolled subjects. Table 2 gives an overview of these analyses, the available datasets, along with their main outcome parameters, structured per objective. More details on each analysis are described in the subsequent sections.

Table 2
Study design based on three objectives.

	Included patients	Muscle	Techniques	(Primary) outcomes
Objectives				
1) SCM alterations				
TD vs CP	TD: n = 13 CP: n = 16	MG	IF labeling, Flow cytometry	**SCM Fusion index (Day 6)**
2) SCM heterogeneity				
2.1 MG vs ST	TD: n = 3 CP: n = 6	MG and ST	FACS, IF labeling Muscle section analysis	FACS fractions, KI67and MYOD quantification, **Fusion index (Day 6)**
2.2 Longitudinal (Pre-post BoNT)	CP: n = 4	MG	FACS, IF labeling	FACS fractions, MYOD quantification **Fusion index (Day 6)**
2.3 Repeatability	TD: n = 2	MG	FACS, IF labeling	FACS fractions, MYOD quantification **Fusion index (Day 6)**
3) Supportive stem cell characteristics (MAB, FAP, IC)				
3.1 MG vs ST	TD: n = 3 CP: n = 5	MG and ST	FACS, IF labeling, Muscle section analysis	FACS fractions, MYOD quantification, **Fusion index (Day 6)**
3.2 Longitudinal (Pre-post BoNT)	CP: n = 4	MG	FACS, IF labeling	Oil Red O quantification FACS fractions, **Fusion index (Day 6)**

SCM: satellite cell-derived myoblast, TD: typically developing, CP: cerebral palsy, BoNT: Botulinum Neurotoxin Type A, n: number, GMFCS: Gross motor function classification scale, MG: medial gastrocnemius, ST: semitendinosus, SC: satellite cell, MAB: mesoangioblast, FAP: fibro-adipogenic progenitors, IC: interstitial cell, IF: immunofluorescence, FACS: Fluorescence activated cell sorting. Primary outcome parameters are indicated in bold.

2.3. Cell culture and stem cell isolation via FACS

Cells were amplified and isolated according to a previous published protocol (Corvelyn et al., 2020). Cell populations were isolated by serial fluorescent activated cell sorting (FACS) using a BD FACSAria II (BD biosciences) or Sony MA9000 (Sony) device. Calcein violet (10μM/1 × 10^6 cells, eBioscience), was used as additional viability control. Firstly, after 3 to 4 *in vitro* passages, satellite cell-derived myoblasts (SCMs) as for the previous data set (Corvelyn et al., 2020)), were sorted based on the single CD56 marker (Tey et al., 2019). CD56 negative cells were further amplified and sorted in order to isolate mesoangioblasts (MABs), based on the presence of Alkaline Phosphatase (CD56- ALP+ PDGFRa- cells), while fibro-adipogenic progenitor cells (FAPs) were sorted for Platelet-Derived Growth Factor alpha (CD56- ALP- PDGFRa+ cells). Interstitial cells (ICs) were collected based on the absence of these markers (CD56- ALP- PDGFRa-). All antibody details are specified in Supplementary Table 1. We will refer to these progenitor populations as SCMs, MABs, FAPs and ICs. All cell populations underwent further proliferation and differentiation assays followed by immunofluorescent labeling as further described.

2.4. Stem cell characterization by flow cytometry analysis

Antibody titrations for FACS optimization and further flow cytometry analyses were performed with a FACSCanto II HTS (BD biosciences). Experiments were performed on unsorted cells of passage 4–6, to prove that the obtained cell population with FACS isolation was pure, based on the absence of significant percentages of stemness marker CD34, haematopoietic marker CD45 and endothelial markers CD144 and CD31. Positive control samples, U266 multiple myeloma cell line and iPSC-derived endothelial cells (De Smedt et al., 2021), were obtained to show the specificity of the antibodies. Data were analyzed with FlowJo v10.6.1 software.

2.5. In vitro differentiation assays

Myogenic (SCMs and MABs) and adipogenic (MABs, FAPs and ICs) differentiation assays were performed as previously reported (Corvelyn et al., 2020) up to 6 and 10 days, respectively. Cells included for proliferation analyses were seeded at a density of 3 × 10^3 cells/cm^2 and analyzed after 0 and 2 days in growth medium. In the light of the repeatability assessments, a subgroup of SC cells (n = 5) underwent myogenic differentiation at different passages (P and P+2).

2.6. Immunofluorescent labeling and imaging of differentiated cells

Cells were cultured in 96 well dishes (Thermo Fisher Scientific) and fixed with 4% paraformaldehyde. Immunofluorescent (IF) labeling was performed according to our previously published protocol (Corvelyn et al., 2020). All used primary antibodies are listed in Supplementary Table 1. Appropriate secondary antibodies were used (1:500, Alexa Fluor® donkey 488 or 594, Thermo Fisher Scientific). Hoechst (1:3000 in PBS, Thermo Fisher Scientific) was used for indicating nuclei. Fusion index (FI) was calculated as ratio between at least 2 myonuclei per Myosin Heavy Chain (MyHC) positive area and the total number of nuclei in a field of view. Three randomized images per well have been analyzed per assessment. Visualization occurred with an Eclipse Ti Microscope (Nikon) and NIS-Elements AR 4.11 software or an inverted DMi8 microscope (Leica) and LASX software, depending on the labeling.

2.7. Oil Red O staining and quantification of adipogenic differentiation potential

After 10 days of adipogenic differentiation, Oil Red O (ORO) staining was performed to assess the deposition of lipid droplets, as previously described (Corvelyn et al., 2020). Cells were incubated for 50 min with ORO solution (65% of 0.5% w/v Oil Red O in isopropanol (Thermo Fisher Scientific) and MQ water). Secondly, the previously described standard IF protocol for cells was applied for visualization of the adipocyte membrane with Perilipin. ORO was measured by extracting lipids with a petrol ether/isopropanol mixture (3:2) and quantified for their absorbance at 490 nm for 0.1 s with Victor Spectrophotometer (PerkinElmer). Standard curve was applied and quantification was expressed in μg of pure ORO powder.

2.8. Histological and immunofluorescent analyses on muscle sections

As a side trajectory, for a subgroup of patients, we included additional microbiopsies to perform histological assessment of the muscle tissue, which allowed to complement the *in vitro* cell culture data and assess the CP muscle in an explorative manner. Muscle microbiopsies were snap-frozen in isopentane cooled in liquid nitrogen and stored at −80 °C. Five μm muscle sections were obtained using a CryoStarTM NX70 Cryostat (Thermo Fisher Scientific) while kept at −20 °C. Haematoxylin and Eosin staining was performed on few ST (n = 3) muscle sections by incubating the slides at RT for 1 min in haematoxylin solution (Merck). Slides were then washed for 10 min in running tap water before incubating for 1 min in eosin solution (Sigma-Aldrich). Slides were then washed extensively in tap water. To dehydrate, sections were incubated consecutively for 10 s in 70%, 90% and 100% ethanol and 5 min in xylene/ethanol (1:1, Merck) and 5 min in xylene. Muscle sections were dried, before mounting with DPX mountaint (Merck) and qualitatively compared via visual assessments for contractile material and extra-cellular matrix.

IF labeling for SC counting on MG and ST muscle slides was performed based on co-localization of PAX7 and Dapi. Sections were placed at room temperature (RT) for 10 min in a humid chamber followed by 10 min fixation in cold acetone. After washing with PBS, slides were incubated with 10% goat serum (Invitrogen) for 1 h. Primary antibodies were applied in blocking solution overnight at 4 °C. After 3 × 5 min washing with PBS, muscle slides were incubated for 1 h at RT with appropriate secondary antibodies (1:500, Alexa Fluor® goat 488 or 680, Thermo Fisher Scientific). After 3 × 5 min washing with PBS, Dapi (1:50 in PBS, Thermo Fisher Scientific) was added for 1 min and the samples were extensively washed with PBS and mounted with ProLong® Gold antifade reagent (Molecular Probes). Visualization was performed with an inverted DMi8 microscope (Leica) and LASX software. An average of 512 fibers (range 197–923) were analyzed for PAX7+ nuclei according to Mackey et al. (2009) for good representation, depending on the sample quality and cross-sectional orientation (Mackey et al., 2009). This counting was normalized per 100 myofibers.

2.9. Data analyses

Data in this study are represented using means ± standard deviation. Boxplots have been used in the visualization of FI values, percentages of KI67+ or MYOD+ nuclei and ORO quantifications. The boxplots indicate the 25th to 75th percentiles, while the whiskers indicate the minimum and maximum values. The centre of the boxplot indicates the median. FACS fractions are indicated by individual values and the bar represents the mean. Unpaired T-tests were performed for comparison between the TD and CP groups (two-tailed, $p < 0.05$). One-way ANOVA was applied to compare FI values of SCMs from TD children and patients with CP with or without the presence of fixed contractures at the level of the MG. Paired T-tests were applied to compare data from the MG and ST muscles as well as for longitudinal comparisons. Data were pooled from CP and TD children, when relevant, and only in case no differences were found between groups. Repeatability assessments were explored in a qualitative way. Analyses of SCM FI values with a difference of two passages was performed using a Two-tailed paired T-test. Numbers of analyzed data are always indicated in the results section as well as in the figure legends. Statistical analysis and simple linear regression analysis

were performed using GraphPad Prism 8 software. Significance of the differences was reported using '$' for TD and CP, '*' for comparison between MG and ST and '§' for assessment prior to and after BoNT treatment and for all of them it represents p-values smaller than 0.05.

3. Results

3.1. Satellite cell-derived myoblast alterations of patients with CP compared to TD (objective 1)

Based on immunofluorescence (IF) images for Myosin Heavy Chain (MyHC) and a nuclear dye, Hoechst, we found higher fusion index (FI) values for satellite cell-derived myoblasts (SCMs) from *Medial Gastrocnemius* (MG) muscle of children with CP (41.60 ± 17.94%; n = 16) compared to those of TD (28.33 ± 14.39%; n = 13; $ $p < 0.05$; Fig. 1). These data (CP: n = 2, TD: n = 8) were added to previous published results (CP: n = 14, TD: n = 5) and implemented with additional TD data to increase power (Corvelyn et al., 2020). No association with fixed contractures (n = 8) and fusion index could be observed in these MG-derived SCMs.

Flow cytometry was performed on the total population of cells extracted from the muscle to quantify additional markers such as markers of stemness (CD34) or markers that are highly expressed by blood cells (CD45) or endothelial cells (CD31 and CD144, TD and CP: n = 6) in order to better quantify the purity of the expanded cells as muscle cells. Analysis showed that on average 1.78 ± 1.97% of all cells were positive for CD34 marker in TD and 0.69 ± 0.88% in CP. On average 0.28 ± 0.30% of cells derived from TD samples and 0.05 ± 0.06% from CP were positive for CD45 haematopoietic marker. The endothelial markers CD144 and CD31, were expressed by 0.03 ± 0.07% and 0.03 ± 0.06% of TD cells and 0.01 ± 0.01% and 0.03 ± 0.03% of CP-derived cells, respectively (Supplementary Figs. 1A and B). No significant differences between TD and CP samples were found, while excluding contaminating populations of endothelial and haematopoietic origin. Positive control sample for haematopoietic cells, U266 lymphocytes, showed 11.5% CD45+ cells and 44.9% CD31+ cells (Supplementary Fig. 1C). Positive control sample for endothelial cells, hiPSC-derived endothelial cells were included and showed expression of markers CD144 by 8.7% and CD31 by 84.8% (Supplementary Fig. 1D). Both control samples showed expression levels according to previous literature (Sidney et al., 2014; Zhou et al., 2004). Overall, we showed higher fusion capacity of the SCs derived from the MG of patients with CP compared to those of TD without the interference of haematopoietic and endothelial cells.

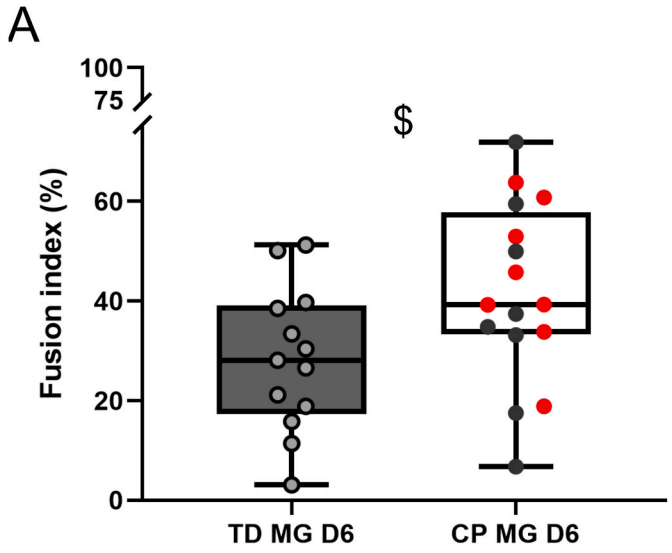

Fig. 1. Fusion index of satellite cell-derived myoblasts from the *Medial Gastrocnemius* (MG) muscle. (A) Fusion indexes of SCM myogenic differentiation at day 6, completed with additional data from both typically developing children (TD) and patients with cerebral palsy (CP). Data shown by boxplots, every dot represents an individual subject. Data from patients with CP with fixed contractures at the level of their *Gastrocnemius* muscles are indicated in red (n = 8). TD: n = 13, CP: n = 16, $ $p < 0.05$.

3.2. Satellite cell heterogeneity based on muscle-specificity (objective 2.1)

Firstly, in order to examine the observed heterogeneity amongst different studies with regard to muscle stem cell behaviour, we have assessed SCMs from two different lower limb muscles (the MG and the *Semitendinosus* (ST)) of the same subjects. FACS analyses showed proportions 38.8 ± 10.78% in TD (n = 3) and 34.05 ± 19.53% in CP (n = 6) for the MG muscle. In the ST muscle, SCMs were represented for 31.33 ± 13.26% in TD children and 25.38 ± 15.92% in CP (Fig. 2A). Since no differences could be found between TD and CP, we pooled the data of both groups as we observed a slight reduced SCM fractions in the ST muscle compared to MG (−8.27%), but this observation failed to reach statistical significance. Additionally, we quantified *ex vivo* satellite cell (SC) representations based on PAX7+ nuclei in muscle sections, as this staining marks quiescent SCs. Correlation assessment of FACS fractions and *ex vivo* SC localization in muscle sections showed no correlation (R^2 = 0.006, n = 12 (pooled TD, CP, MG and ST data); Supplementary Fig. 2).

SCMs (CD56+) were analyzed for the expression of KI67, a proliferation marker, based on IF labeling at day 0 and day 2 during proliferation conditions (Fig. 2B and C). No differences between TD and CP nor between both muscles, were found on both time points. SCMs underwent myogenic differentiation and were analyzed for MYOD protein expression and fusion index (FI) at days 3 and 6 of differentiation (Fig. 2D–F). No differences were found when MYOD, a marker for activated myogenic precursors, was quantifiied for both groups and muscles at days 3 and 6. Secondly, FI analysis showed no significant differences in the ability of these SCMs to fuse into myotubes between TD and CP at any time point. However, the FI values tended to be higher in the MG-derived SCMs compared to those of the ST at both time points for both groups. More specifically, FI values significantly increased in MG compared to ST at day 6 (MG: 42.78 ± 6.36%; ST: 31.42 ± 4.96%) for TD (n = 3; *$p < 0.05$). This increased FI was also reported as significant at day 3 for CP (MG: 40.61 ± 11.43% and ST: 25.62 ± 11.49%; n = 6; *$p < 0.05$). As no significant differences were primarily present between TD and CP in this dataset, we secondarily pooled data of the MG and ST from all subjects (TD and CP, n = 9) to better explore potential muscle-specificity. SCMs derived from the MG muscle had higher FI values compared to those of ST both at days 3 (MG: 38.87 ± 10.67% and ST: 25.08 ± 9.19%; $p = 0.010$) and day 6 (MG: 44.14 ± 12.75% and ST: 32.66 ± 12.65%; $p = 0.012$). Taken together, we found higher fusion capacity of SCMs derived from the MG compared to the ST for both the TD as well as the CP group during myogenic differentiation.

3.3. Longitudinal effects on stem cell features from the MG of patients with CP (objective 2.2)

Secondly, to examine possible effects of the Botulinum Neurotoxin A (BoNT) treatments and/or the natural pathway of the clinical picture of the CP pathology on the muscle stem cells, four patients with CP were enrolled twice for assessing MG microbiopsies, prior to BoNT treatment (BoNT naive) and post BoNT treatment (BoNT treated). No significant differences in SCM FACS fractions in patients with CP were observed comparing time points prior to and after BoNT treatment, although an average decrease of 16.4% was found (Fig. 3A). Myogenic capacity of these SCMs indicated that three out of 4 cases showed a lower percentage of MYOD+ nuclei and FI values after BoNT treatment, while in one case, both parameters were slightly higher at day 6 (Fig. 3B–F). In general, SCM MYOD+ nuclei decreased on average with 5.34% and FI

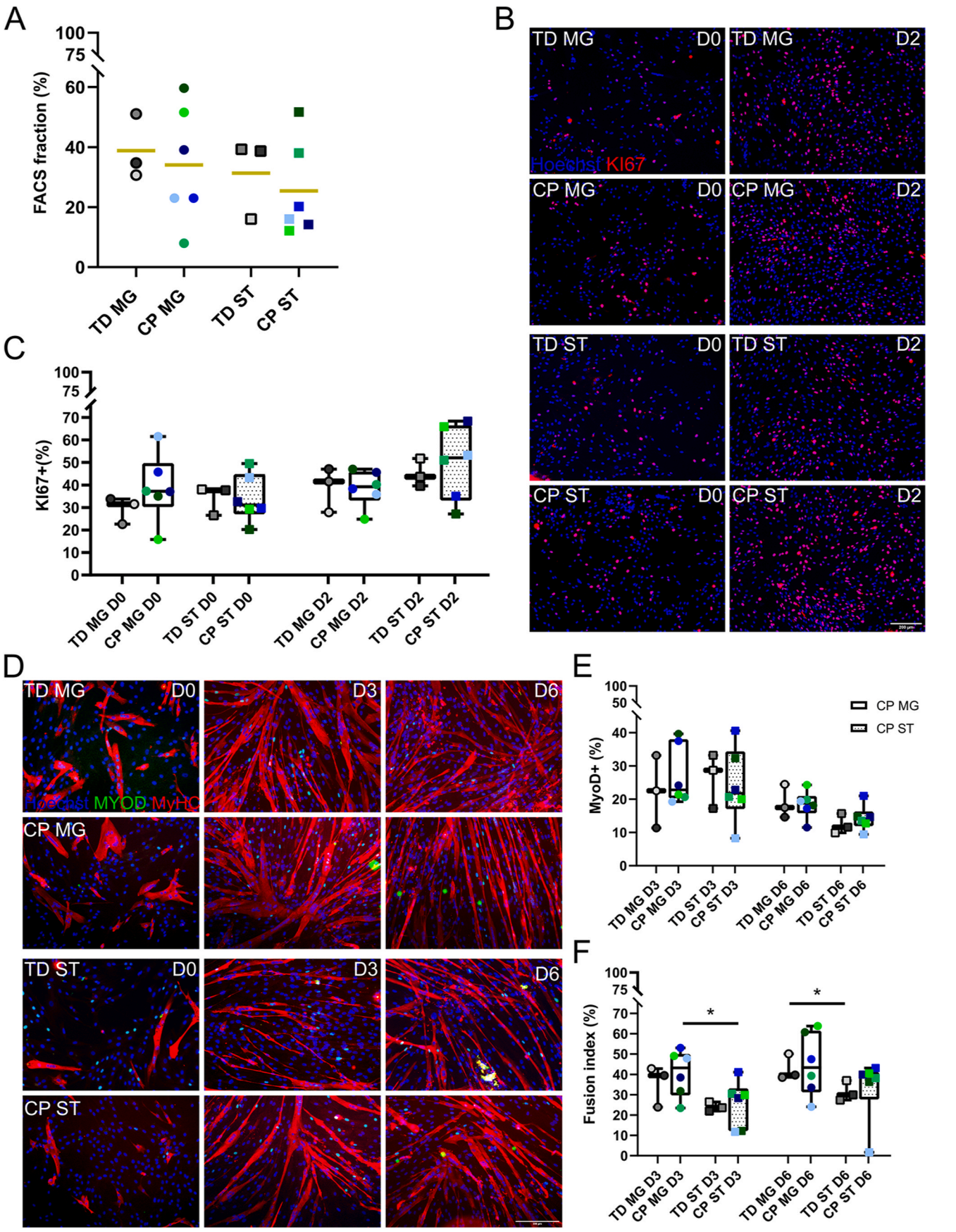

(caption on next page)

Fig. 2. Satellite cell-derived myoblast features of the *Medial Gastrocnemius* (MG) and *Semitendinosus* (ST) muscle in TD and CP children. (A) Fraction of obtained stem cells through FACS with CD56 marker, referred to as SCMs. Data expressed as percentage of total sorted cells. The bar represents the mean. Dots (MG) and squares (ST) represent individual subjects indicated in different colours. **(B)** Representative immunofluorescent (IF) images from SCMs derived from TD children and patients with CP for both MG and ST muscle at day 0 and day 2 during proliferation. KI67 is shown in red. Nuclei (blue) are counterstained using Hoechst. **(C)** Percentage of KI67 positive cells based on IF images. Data shown by boxplots, dots (MG) and squares (ST) represent individual subjects indicated in different colours. **(D)** Representative IF images from SCMs derived from TD children and patients with CP for both MG and ST muscle at days 0, 3 and 6 of myogenic differentiation. MYOD (green) and Myosin Heavy Chain (MyHC; red) are shown. Nuclei (blue) are counterstained using Hoechst. **(E)**. Percentage of MYOD+ cells based on IF images represented by boxplots for SCMs from both TD children and CP patients. Dots (MG) and squares (ST) represent individual subjects indicated in different colours. **(F)** SCM fusion indexes shown by boxplots. Dots (MG) and squares (ST) represent individual subjects indicated in different colours. Scale bars are 200 μm. TD: $n = 3$, CP: $n = 6$, *$p < 0.05$.

values decreased on average with 9.71% in comparison to the pre-BoNT time point after 6 days of myogenic differentiation.

3.4. Repeatability and reliability of the assessed outcome parameters (objective 2.3)

Thirdly, to explore to what extent the observed findings could be influenced by the procedure or biopsy quality, two separate micro-biopsies of the MG from TD children were obtained at the same time and at the same muscle location and processed in parallel ($n = 2$). FACS fractions for the CD56+ population fluctuated by 24.23% between repeated assessments (Supplementary Fig. 3A). For the myogenic parameters, percentages of MYOD+ nuclei and FI values remained stable at days 3 and 6, but showed rather high heterogeneity at day 0 (Supplementary Figs. 3B and C). On average a minor difference between repeated assessments of 4.66% was observed at day 3 and 1.59% at day 6 for MYOD protein expression, while FI differed with 2.45% and 7.46% at days 3 and 6, respectively. To this end, the full analysis including day 0 (which has shown to be less robust) for MyoD protein expression and fusion index has been included in Supplementary Figs. 3D and E.

In this light, we determined the effect of these SCM FACS fluctuations on the FI measured at day 6 of myogenic differentiation by simple linear regression on the full dataset, including both TD ($n = 13$) and CP ($n = 16$) data (Supplementary Fig. 3F). There was no correlation between SCM FACS fractions and the FI measured at day 6 of myogenic differentiation ($R^2 = 0.1781$). Furthermore, the effect of variance in passage number of SCMs at the time of myogenic differentiation was assessed as this could vary with maximum two passage numbers within the full dataset or within the longitudinal measurements prior to and after BoNT treatment. SCMs were differentiated towards myotubes and FI was calculated at two time points with a difference of two passage numbers: no significant alterations of the fusion index at day 6 were reported ($n = 5$; Supplementary Fig. 3G).

3.5. Characterization of supportive stem cell populations in MG and ST muscles (objective 3.1)

There were no differences between MAB fractions (PDFGRa- ALP+) of TD (MG: 14.27 ± 12.63% and ST: 4.39 ± 4.48%; $n = 3$) and CP (MG: 15.83 ± 15.16% and ST: 2.27 ± 1.73%; $n = 5$; Fig. 4A). However, a higher MAB proportion was found in the MG muscle compared to ST muscle when pooling data from TD and CP children ($n = 8$, $p = 0.020$). FAP fractions (ALP- PDGFRa+) were scarcely represented and showed no significant differences between TD (MG: 0.19 ± 0.12% and ST: 2.78 ± 4.17%; $n = 3$) and CP (MG: 0.62 ± 0.69% and ST: 0.87 ± 0.88%; $n = 5$), nor between muscles (Fig. 4B). Fractions of ICs (CD56- ALP- PDGFRa-) were represented with 47.48 ± 5.43% in the MG and 63.37 ± 5.05% in the ST for TD ($n = 3$) and 36.32 ± 20.86% in the MG and 45.13 ± 23.40% in the ST for CP ($n = 5$; Fig. 4C). ICs representation was higher in the ST muscle compared to MG ($n = 8$, $p = 0.009$).

Myogenic differentiation potential of MABs at day 6 of differentiation showed no differences between TD and CP based on MYOD protein expression and FI values for both muscles (Fig. 5A–C). The comparison of MG and ST revealed a significant increase of MYOD+ nuclei in the TD group for the MG (16.44 ± 4.32%) compared to the ST (4.96 ± 2.45%; $n = 3$; **$p < 0.01$), while no differences were reported in the CP group (MG: 17.89 ± 16.33%; ST: 10.87 ± 9.26%; $n = 5$). A high heterogeneity for FI values of the MABs was observed within the CP group and no differences were found between the TD and CP group, nor between both muscles. After adipogenic differentiation of these MABs, similar amounts of lipid content were found for both groups and muscles, while adipogenic capacity slightly increased in the ST muscle of CP compared to TD, but this increase did not reach statistical significance ($p = 0.188$; Fig. 5D and E). FAPs were assessed for adipogenic differentiation potential (Fig. 5F and G), as it was previously shown that they do not possess myogenic capacity by themselves (Corvelyn et al., 2020). No differences between TD and CP groups nor between muscles were found, based on ORO quantification. Lastly, ICs (ALP- PDGFRa-) have been assessed for their adipogenic capacity and did not show any significant differences based on ORO quantification between groups nor between muscles (Fig. 5H and I). Taken together, we found altered stem cell representations comparing the MG and the ST, with a higher myogenic commitment of the MABs from the MG compared to ST, although no differences in adipogenic potency between muscles nor patient groups were observed.

Of note, for the ST muscle, ICs of one specific patient with CP showed aberrant high adipogenic potency *in vitro* based on ORO quantification. This finding linked to the visual assessment of histological muscle sections stained with haematoxylin and eosin (Supplementary Fig. 4). Thereby, a qualitative comparison of the ST muscle from a TD child and from another CP child, with average ORO levels for IC adipogenic differentiation, could be made. A higher accumulation of fibrosis and/or fatty infiltration was observed by increased connective tissue between the muscle fibers for the sample from this specific CP patient with high IC adipogenic potential. This in comparison to the TD sample and the one CP sample with average ORO values.

3.6. Longitudinal effects on supportive muscle stem cells (objective 3.2)

Examining the effects pre- and post BoNT treatment on the supportive muscle stem cells from CP children showed no differences in FACS fractions for MABs (CD56- ALP+ PDGFRa- cells; $n = 4$), but revealed a significant decrease for FAPs (CD56- ALP- PDGFRa+ cells; BoNT naive: 9.13 ± 4.16%; BoNT treated: 1.04 ± 0.89%; §$p < 0.05$) and an increase for ICs (CD56- ALP- PDGFRa- cells; BoNT naive: 10.20 ± 8.62%; BoNT treated: 42.08 ± 13.65%; §$p < 0.05$; Fig. 6A–C). Based on the repeatability experiments ($n = 2$), we found that FACS fractions stayed rather consistent for these stem cell populations (average fluctuations between repeated assessments for MABs: 6.44%; FAPs: 0.16% and ICs: 14.25%; Supplementary Fig. 5A). To verify whether this small sample size is representative, we portrayed these longitudinal data together with the cross-sectional results of the entire study group. Thereby individual changes between the two timepoints of the subgroup could be compared to the baseline variability amongst all CP children and TD subjects (CP BoNT naive: $n = 6$; CP BoNT treated: $n = 9$; TD: $n = 13$; Supplementary Figs. 5B and C). Additional simple linear regression of these fractions and age was performed on a cross-sectional dataset in an attempt to understand whether these alterations could be due to maturation, the natural pathway of the clinical CP picture or associated with BoNT treatment history (Supplementary Figs. 5D and E). No link

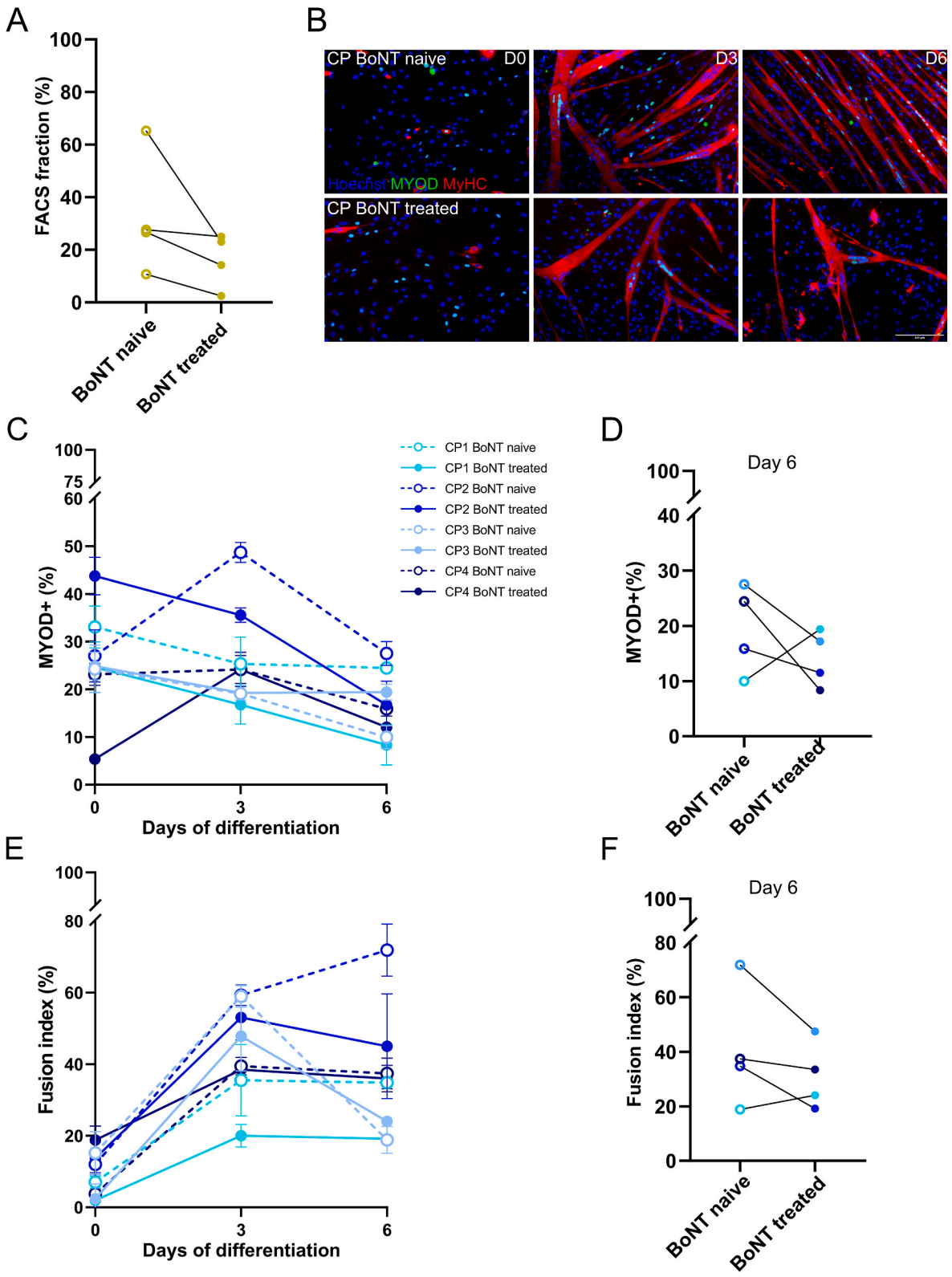

Fig. 3. Satellite cell-derived myoblast features prior to (BoNT naive) and post Botulinum toxin treatment (BoNT treated). (A) Quantification of SCMs from the MG, expressed in percentage of total sorted cells from patients with CP prior to (BoNT naive) and post (BoNT treated) BoNT treatment. (n = 4) **(B)** Representative IF images of CP patient-derived SCM myogenic differentiation at days 0, 3 and 6 from a BoNT naive patient and at one year after BoNT treatment. MYOD (green) and MyHC (red) and nuclei (blue) are shown. Scale bar = 200 μm. **(C)** Percentages of MYOD+ cells based on IF images for SCMs from both TD children and CP patients. Error bars indicate the standard deviation per measurement. Each subject is indicated in a different colour indicated by the figure legend. SCMs from BoNT naive patients with CP are indicated by dotted lines and by solid lines after BoNT treatment. **(D)** Longitudinal effect on MYOD nuclear protein expression in SCMs at day 6. Data from the same subject are connected through a black line from BoNT naive to BoNT treated. **(E)** Fusion indexes of SCMs from patients with CP at days 0, 3 and 6 of myogenic differentiation. Each subject is indicated in a different colour. Error bars indicate the standard deviation per measurement. **(F)** Longitudinal effect on FI of SCMs at day 6. Data from the same subject are connected through a black line from BoNT naive to BoNT treated.

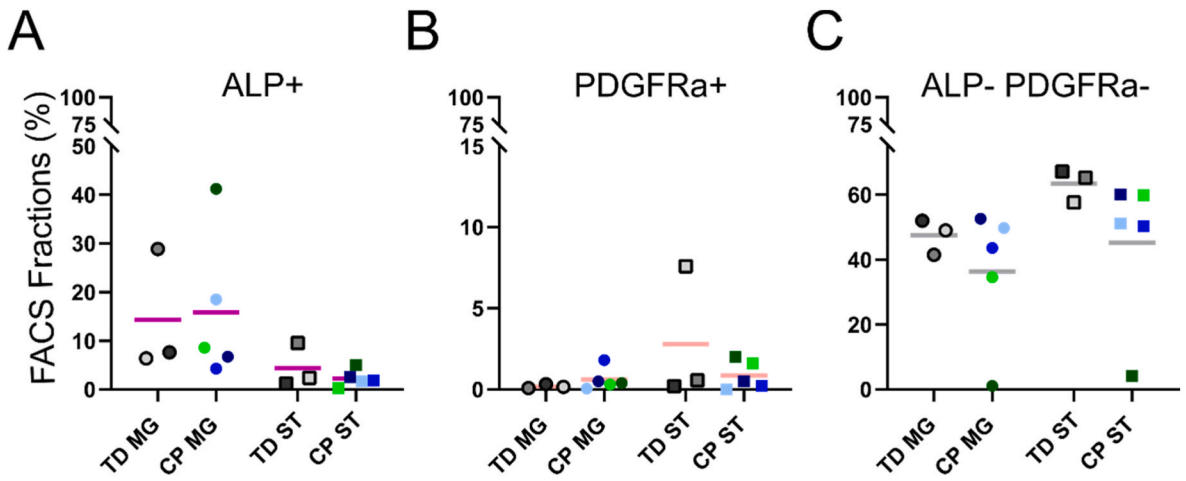

Fig. 4. FACS fractions of isolated supportive stem cell populations obtained from the MG and ST muscle in TD and CP children. (A) Percentages of obtained CD56- PDGFRa- ALP+ cells based on a serial FACS, referred to as mesoangioblasts (MABs). Data expressed as percentage of total sorted cells. The bar represents the mean. **(B)** Percentages of obtained CD56- ALP- PDGFRa+ cells, referred to as fibro-adipogenic progenitor cells (FAPs), through FACS analyses. **(C)** Percentages of obtained CD56- ALP- PDGFRa- cells, referred to as interstitial cells (ICs), through FACS. Every dot represents data from a different subject, typically developing (TD) children or patients with cerebral palsy (CP) according to the colour code. Cell populations derived from muscle microbiopsies from the MG are indicated by circles, populations from the ST are indicated by squares. The horizontal line represents the mean. TD: n = 3, CP: n = 5.

with age or BoNT treatment history could be found (n = 11).

Furthermore, to have a complete overview of myogenic capacity prior to and after BoNT treatment, we assessed MAB myogenic differentiation at day 6. This revealed a steep increase in FI in two out of four cases, but a decrease in fusion potential for the other two cases (Fig. 6D and E).

4. Discussion

Through the current study three predefined objectives could be achieved. First, we confirmed higher satellite cell-derived myoblast (SCM) fusion potential from the *Medial Gastrocnemius* (MG) of CP compared to age-matched TD children. Secondly, we reported a decreased myogenic differentiation potential of SCMs from the *Semitendinosus* (ST) compared to the MG muscle based on fusion indexes from pooled CP and TD data. Furthermore, based on longitudinal assessments, we showed slightly reduced SCM representation and differentiation potential, one year after the first BoNT treatment. Thirdly, mesoangioblasts (MABs) revealed to be less represented in the ST compared to the MG muscle. Finally, we also described alterations in FACS fractions of supportive stem cell populations after Botulinum Neurotoxin A (BoNT) treatment.

4.1. Increased satellite cell-derived myoblast fusion capacity in CP compared to TD (objective 1)

Related to the first objective, i.e., comparing SCMs from typically developing (TD) children with those of patients with cerebral palsy (CP), we reported higher fusion index (FI) values at day 6 for SCMs derived from the MG microbiopsies of young patients with CP compared to age-matched TD children. Thereby, we confirmed our previously published results on SC-derived cultures (Corvelyn et al., 2020). These *in vitro* findings suggest that these SCMs, given the right cellular environment, would still be able to contribute to muscle growth and regeneration *in vivo*, in contrast to what is observed in for example Duchenne muscular dystrophy (Choi et al., 2016). Although very variable results in previously published studies, assessing different muscles and sometimes lacking ideal control data, based on RNAseq analyses on muscle biopsies have indicated upregulation of pathways related to muscle protein synthesis, such as *ACTA1* and *MYL1* indirectly supporting our data on SCM differentiation (Robinson et al., 2021; Smith et al., 2012). However, next to SCM fusion potential, we hypothesize that alterations in myotube morphology and nuclear positioning, as was previously described (Corvelyn et al., 2020), could have an effect on the muscle functioning. For instance, multiple studies analyzing these *in vitro* myoblast features have described similar large myotubes and myonuclear aggregations in diverse myopathies leading to muscle weakness (Azevedo and Baylies, 2020; Chal et al., 2015; Fernandes et al., 2020). Further research is needed to better quantify these features and its potential implications on the muscle functioning. Additionally, we have further characterized all cells obtained via the muscle microbiopsy technique that resulted negative for haematopoietic and endothelial cell markers, addressing the concerns about the SCM purity recently raised by Lieber and Domenighetti (2021). These findings were in line with previous reported data, even on additional markers for cells obtained from muscle microbiopsies followed by the explant technique (Ceusters et al., 2017). Small percentages of cells have been found positive for CD34, which is mainly known as a marker for adult stem cells including a small subset of SCs (Tey et al., 2019). Moreover, cells positive for CD34 have been previously reported after culturing muscle microbiopies (Ceusters et al., 2017; Sidney et al., 2014). Thereby, we provided evidence that the cells analyzed were not being contaminated by considerable amounts of cells of other lineages.

4.2. Satellite cell-derived myoblast features from patients with CP are influenced by multiple variables (objective 2)

To address the second study objective, we assessed multiple factors potentially leading to heterogeneity in reported results on the CP muscle pathology (Corvelyn et al., 2020; Domenighetti et al., 2018; Handsfield et al., 2022). Firstly, to address objective 2.1, we have uniquely cultured and extracted cells from two different muscles of the same young patients with CP, as well as from aged matched TD children. Both, the MG and ST (or entire group of hamstring) muscles have been described at the macroscopic level, i.e. muscle volume via ultrasound assessments and at the microscopic level, i.e. contractile material and collagen content in muscle sections (Howard et al., 2022; Modlesky and Zhang, 2020; Smith et al., 2011), however, rarely from the same subject. Additionally, the majority of previous studies focussed on the entire group of hamstring muscles, without discriminating between the different muscles of the hamstrings (Domenighetti et al., 2018; Htwe et al., 2017; Smith et al., 2011), as targeting i.e. the ST specifically is more challenging to collect

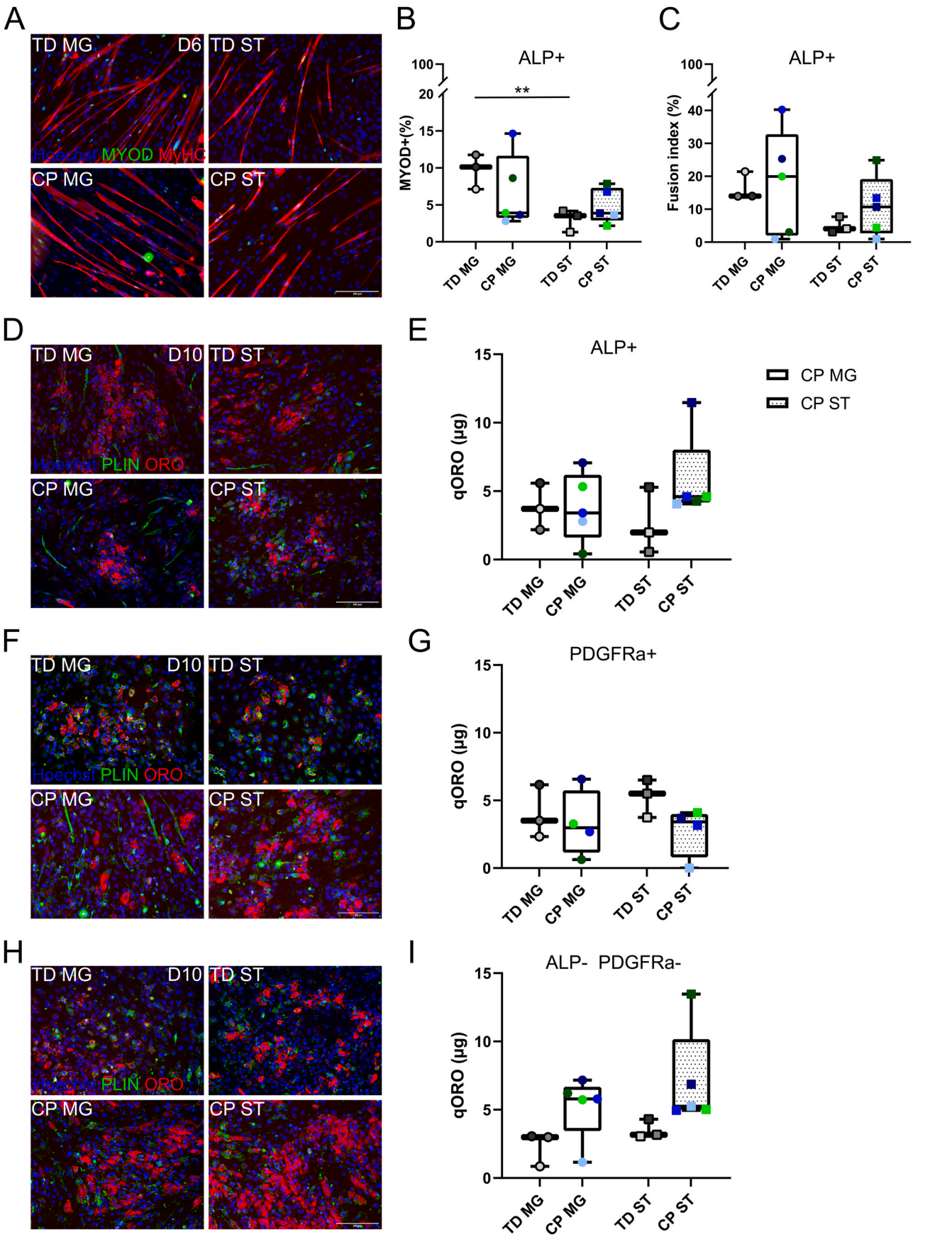

(caption on next page)

Fig. 5. Differentiation potency of MABs, FAPs and ICs from MG and ST muscles of TD children and CP patients. (A) Representative IF images from MABs derived from TD children and patients with CP for both MG and ST muscle at day 6 of myogenic differentiation. MYOD (green) and MyHC (red) are shown. Nuclei (blue) are counterstained using Hoechst. **(B)** Percentage of MYOD+ cells based on IF images represented by boxplots for both TD children and CP patients. Dots (MG) and squares (ST) represent individual subjects indicated in different colours. $^{**}p < 0.01$ **(C)** MAB (ALP+) fusion indexes shown by boxplots. Dots (MG) and squares (ST) represent individual subjects. **(D)** Representative IF images and **(E)** quantification of ORO based on absorbance at 490 nm of MABs from TD children and patients with CP from both MG and ST muscle after adipogenic induction at day 10. Perilipin (PLIN, green), Oil red O (ORO, red) are shown. Nuclei (blue) are counterstained using Hoechst. Data expressed in μg of ORO based on a standard curve. **(F)** Representative IF images and **(G)** quantification of ORO of FAPs (PDGFRA+) from TD children and patients with CP from both MG and ST muscle after adipogenic induction at day 10. PLIN (green), ORO (red) and nuclei (blue) are shown. **(H)** Representative IF images and **(I)** quantification of ORO of ICs (ALP- PDGFRA-) from TD children and patients with CP from both MG and ST muscle after adipogenic induction at day 10. PLIN (green), ORO (red) and nuclei (blue) are shown. Scale bars = 200 μm. TD: n = 3, CP: n = 5 (FAP: n = 4).

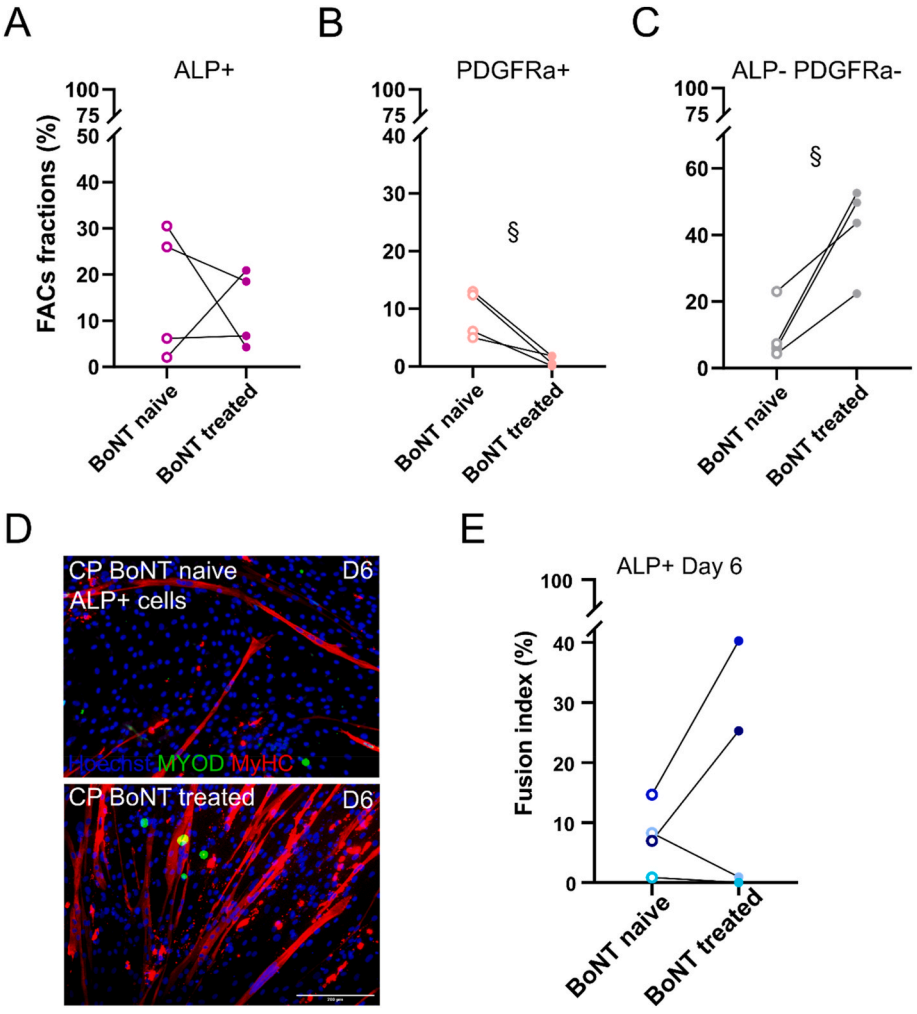

Fig. 6. Longitudinal effects on supportive stem cell representations and myogenic capacity in CP children. (A) Quantification of serial FACS for MABs (ALP+) from the MG, expressed in percentage of total sorted cells. **(B)** Quantification of fibro-adipogenic progenitor cells (PDGFRa+) from the MG, expressed in percentage of total sorted cells. **(C)** Percentages of obtained ICs (ALP- PDGFRa-). Samples from 4 patients with CP were included before the first Botulinum Neurotoxin A (BoNT) treatment, as well as one year after. Every dot represents an individual subject indicated in different colours. n = 4, §p < 0.05 **(D)** Representative IF images of MABs from patients with CP at day 6 of myogenic differentiation. MYOD (green) and MyHC (red) and nuclei (blue) are shown. Scale bars = 200 μm. **(E)** Fusion indexes of MABs from patients with CP at day 6 of myogenic differentiation. FI of MABs from BoNT naive patients are indicated by dotted lines, after BoNT treatment by solid lines. Colour codes indicate the different subjects (n = 4), all cells were obtained from the MG muscle.

sufficient material due to its smaller size. Thanks to the less invasive character of the muscle microbiopsy technique, we were able to collect and compare muscle samples from young patients with CP, as well as TD children, on stem cells from both muscles, MG and ST, in the same child. This is unique and seems more challenging to achieve with Bergström biopsies or open biopsies during invasive surgery (Bergström and Edwards, 1979; Howard et al., 2022). Here, the focus was primarily on the comparison of data from both muscles, and not anymore on the difference between CP and TD data. Comparison of both muscles showed a tendency of lowered amounts of SCMs (based on FACS fractions) in the ST compared to MG. These tendencies in FACS fractions could be partially elucidated by the activity level of these patients prior to the biopsy (Chen et al., 2020; Snijders et al., 2015). Indeed, physical activity could explain whether these cells were activated and stimulated to self-renew or not as the MG and ST differ in fiber distribution and thereby regeneration potential (Sharma et al., 2019; Zimowska et al., 2017). Unfortunately, based on their level of physical activities and hobbies, no clear distinctions between the subjects could be made. Additionally, the MG is highly targeted for stretching by physiotherapy and the use of ankle-foot orthoses (Hösl et al., 2015), which was indeed also the case in our patient cohort. Possibly, these differences in muscle management between both muscles could have an effect on the observed FACS fractions and other assessed parameters. However, since the slight fluctuations in SCM fractions between TD and CP were equally represented in MG compared to ST, we assume that SCM *in vitro* amplification was not altered. Possible stimuli from the stem cell niche, or from other cell types, were diminished once the cells were removed from their muscle environment as they were first amplified for 4 passages in culture before sorting, which could have resulted in no significantly altered SCM fractions in our study design (Chen et al., 2020; Cornelison, 2008). Furthermore, studies have reported reduced SC numbers in patients with CP from 10 years of age onwards in different muscles (hamstrings,

Gracilis and biceps) (Dayanidhi et al., 2015; Smith et al., 2011; Von Walden et al., 2018). Yet, no data are available on the age of onset of this phenomenon and on the underlying mechanisms that may potentially exhaust the cells, as is observed in muscular dystrophies (Chang et al., 2016). Additionally, based on IF muscle sections, we could not confirm a lower amount of SCs in CP compared to TD, possibly due to the low sample size and the inclusion of younger subjects. We also did not observe a correlation of *ex vivo* PAX7+ cells with the obtained FACS fractions after *in vitro* amplification. Potentially, the *in vitro* growth conditions could have altered the absolute cell representations as first FACS analyses could only be performed after at least 3 passages, but allow describing rather relative cell representations. Furthermore, it is known that a cell, after extraction, cannot maintain all the molecular and functional properties owned *in vivo* (Saccone et al., 2014; Sharifiaghdas et al., 2011). Additionally, both methods used a different marker (PAX7 or CD56), which could also be attributed to the discrepancies here described, as PAX7 is rather associated to quiescent SCs and downregulated when the SCs are committed towards differentiation, a state that is more associated with upregulation of CD56 (Snijders et al., 2015). However, as the expansion method was standardized for all cell lines and included subjects, possible effects on proliferation potential would have led to altered FACS fractions when comparing CP and TD data. Additionally, as mentioned before, even though the cells have been removed from their niche, effects of the *in vivo* situation or of the CP pathology might have influenced their ability to still proliferate *in vitro* (Yin et al., 2013). In this light, even though no direct associations between these *ex vivo* and *in vitro* data could be made, both these data suggest that SC representation was not altered in these patients. The absence of significant alterations supports the hypothesis that, in our cross-sectional study, none of the cell populations within CP muscles were exhausted compared to TD muscles.

We did not find any differences in proliferative capacities of SCMs based on KI67 protein expression between TD and CP nor between muscles. KI67 is a commonly used marker for proliferation and is expressed during phases G1, S and G2 of cell cycling, but is absent in resting cells, in G0 (Mackey et al., 2009; Tan et al., 2021). Hereby, we showed a stable proliferation by similar percentages of cells with nuclear protein expression of KI67 over two days in growth medium, probably due to the optimal growing conditions. KI67 protein expression is an indication for the number of cells that are actively involved in cell proliferation, but does not provide information on cell cycling speed, for which more in-depth cell cycle analyses would be required. Previously, another research group showed reduced doubling time for myoblast progenitors derived from hamstring biopsies from patients with CP compared to those of TD adolescents, and higher *KI67* levels based on RNAseq data (Sibley et al., 2021). Furthermore, they also stressed the importance of the site for tissue harvesting. They obtained biopsies at the myotendinous junction, which is reported to be richer in proliferating SCs and primarily involved in SC activation and fusion (Allouh et al., 2008; Kim et al., 2020). In contrast, in the current study, muscle microbiopsies were obtained at the muscle mid-belly, contributing to the reported discrepancies between studies (Corvelyn et al., 2020; Domenighetti et al., 2018). As for myogenic commitment, we found significant higher percentages of MYOD+ nuclei at day 0 of myogenic differentiation in ST SCMs compared to MG for TD children, while the opposite trend was found for patients with CP. However, we showed high variance in both MYOD levels and FI values at day 0 between the repeated biopsy samples of two TD children, while these parameters at days 3 and 6 showed to be more robust, letting less conclusive data at day 0. We found significantly lower FI values for the cells extracted from the ST compared to the MG, suggesting lower myogenic potency of these SCMs. Interestingly, we measured a FI of around 25% at day 3 of myogenic differentiation of CP-derived SCMs from the ST, which is close to the FI value (21%) found by Domenighetti and colleagues after 42h of myogenic differentiation of hamstring myoblasts, regardless many differences in the analysis procedure (Domenighetti et al., 2018). Due to differences in material quantity from the biopsy, Domenighetti group was able to assess myogenic capacity at a younger passage (P4), while we had a longer amplification time and assessed SCM differentiation potential at passage 6–8. Differences between the study of Domenighetti group and the current study for the FI values of TD children could potentially be linked to higher age (14 ± 2 years old) and clinical history (ACL reconstructive surgery) and therefore to a potential misuse or altered activity of the muscle. Unfortunately, to our knowledge, no data are available on SCM fusion capacity of healthy subjects of this young age and *in vitro* passage number. Taking the small sample size and heterogeneity of the CP pathology into account, we carefully suggest altered SCM features from the MG compared to the ST (Corvelyn et al., 2020; Domenighetti et al., 2018), hereby highlighting the complexity of CP muscle pathology and rising caution regarding generalized treatment based on muscle-specific findings.

Secondly, although the application of the muscle microbiopsy technique has some previous mentioned limitations, this technique allowed unprecedented follow-up microscopic assessments (to address objective 2.2). Because of the low sample size (partially due to the covid-situation), associations with the BoNT treatment history or the natural pathway of the clinical picture of the CP pathology cannot yet be fully explored. Nevertheless, the preliminary results provide some unique first insights in possible alterations over time following the same subject. The number of SCMs showed a non-significant decrease one year after BoNT treatment. As was previously shown for SC-derived progenitors of patients within this age range, no correlation with fusion index and age was found (Corvelyn et al., 2020). Although additional data are needed, and potential effects due to activity levels could not be excluded, this preliminary observation is most likely patient-specific and potentially the result of the natural CP pathway or the effect of BoNT treatment. Furthermore, myogenic capacity of SCMs seemed to have slightly decreased one year after BoNT treatment. This decrease exceeded the repeated assessment variability. As shown, this effect of lower fusion capacity was not associated with the observed lower SCM FACS fraction.

Thirdly, to address potential concerns about the assessed outcome parameters, we have performed analyses of two separate muscle biopsies from the same muscle in parallel (objective 2.3). Even though we saw some slight fluctuations in the SCM fractions obtained through FACS leading to varying SCM yields, the effect on the differences of FI remained low, as we could analyze this parameter within a range of two passages after amplification. Importantly, the differences observed between repeated assessments were lower than the observed differences between TD and CP and between both timepoints during the follow-up, strengthening the fact that the observations we highlight are due to the pathology and not to any other secondary factor.

4.3. *Supportive muscle stem cells are not highly altered in patients with CP (objective 3.1)*

To address the third study objective, we could successfully obtain multiple muscle stem cell populations next to SCMs, based on well-described markers in literature (Corvelyn et al., 2020; Tey et al., 2019). These results need to be interpreted with caution due to the low sample sizes and the high heterogeneity observed, mainly in the CP group. For both groups, the number of obtained MABs seemed to be lower in the ST compared to the MG muscle, but was not upregulated in CP compared to TD children. This is in contrast to findings in (older) patients with muscular dystrophy disorders (Dellavalle et al., 2011; Díaz-Manera et al., 2012). In this regard, we also did not observe a rescue in higher MAB fractions in cases of relatively lower SC numbers (Dellavalle et al., 2011; Díaz-Manera et al., 2012; Kuang et al., 2008; Tedesco et al., 2017). Further research on larger sample sizes are needed to better understand whether these observations were due to a lack in power or were depending on the age of the enrolled children. However, these data further strengthen the hypothesis of muscle-specific properties and thereby raise caution in interpretation of previous studies

considering an entire muscle group or lacking appropriate control data.

The myogenic capacity of MABs, both by MYOD protein expression and FI, was significantly lower comparing ST-derived cells from TD children and those of the MG. No differences in FI between TD and CP nor between both muscles were found. However, in the same line as what was found for SCMs, there was a trend of lower myogenic capacity in the ST for the TD group, while these observations were not confirmed in the CP group, most likely due to higher heterogeneity. Additionally, we did not observe any correlations between the myogenic performance of the SCs and the MABs of the same subjects based on MYOD or FI assessments. Adipogenic potency of these cells did not differ between TD and CP nor between muscles, which was also the case for FAPs and ICs. However, muscle imaging studies on patients with CP have shown higher adipose content in the MG muscle compared to TD subjects in children and adults (D'Souza et al., 2020; Svane et al., 2021). Potentially, the subjects in our study were too young to already capture these alterations (*in vitro*), knowing that only a 4% increase in fat fraction was reported in the MG of 8–15-year-olds CP compared to TD (Akinci D'Antonoli et al., 2021). ICs showed a slight trend of higher adipogenic capacity for the ST muscle compared to the MG, in both groups. This finding may potentially be in line with greater muscle volumes deficits observed in the distal lower limb muscles compared to more proximal ones, as more fat infiltration could compensate potential changes in total muscle volume (Modlesky and Zhang, 2020). Furthermore, adipogenesis seemed to be linked to a certain location along the muscle, as significant increased fat content was mainly observed at the muscle belly of the MG of more affected patients with CP (D'Souza et al., 2020). Additionally, in our dataset, one IC cell line from the ST of a patient with CP seems to have a much higher adipogenic potency compared to the other ICs obtained from ST in the CP group that was confirmed on qualitative assessment of histological showing a higher extracellular matrix (ECM) content between the muscle fibers. This assessment included histological imaging of a representative TD and a second patient with CP (matched on GMFCS level and gender and having a similar strength score). Interestingly, however based on this single observation, a higher ECM content was observed for the patient with repetitive BoNT treatments and slightly older in age (22 months) compared to the other patient with CP, which only received one previous BoNT treatment. More quantitative data as well as more specific labeling for fat infiltrations would be required to give robust associations to our described single case. More specific investigations will be able to give a better interpretation of these observations, seen the importance of understanding fat infiltration mechanisms together with progression of this as many other diseases affecting skeletal muscle.

4.4. Longitudinal effects on supportive stem cells pre- and post BoNT in patients with CP (objective 3.2)

Based on the FACS data of all four patients, we showed a significant decrease in FAP fraction and an increase in IC fraction in CP children after one year. It has been shown that, in chronic atrophic conditions caused by motor neuron deficits, increased fibrosis is associated with accumulation of FAPs in the interstitium of denervated muscles (Biferali et al., 2019; Contreras et al., 2016; Madaro et al., 2018). This seemed not to be the case by our FACS fractions, even though the CP pathology is expected to be characterized by increased fibrotic content (Howard and Herzog, 2021). The included subjects may have been too young to already notice differences in active involvement of these stem cell populations as we currently do not know at which age this accumulation in ECM occurs in the muscle and if it occurs differently from muscle to muscle. Additionally, as ICs are defined by negative expression for markers CD56, ALP and PDGFRa, possible intrinsic differences in this mixed population remained unnoticed. The reduction in PDGFRa population (FAPs) could have contributed to the increase of the IC population, potentially incrementing ECM deposition (Shadrin et al., 2016). Moreover, alterations in PDGF signaling could modulate multiple processes in cell survival, cell fate decisions and damage-associated behaviours in the muscle, contributing to the observed CP muscle pathology (Contreras et al., 2021).

5. Conclusion

This study confirmed our previous findings that satellite cell-derived myoblast (SCM) cultures derived from the *Medial Gastrocnemius* (MG) muscle of young patients with cerebral palsy (CP) have a higher fusion capacity compared to those of age-matched peers. Through enlarging the TD sample size, clarifying the sample identity and refining the sample homogeneity, we obtained results that are in line with what was previously published (Corvelyn et al., 2020). Parameters were proven to be quite robust based on repeatability experiments assessing SCMs in parallel from the same subject and muscle. To better understand the current heterogeneity in literature, for the first time, we obtained cells through the muscle microbiopsy technique from two different lower limb muscles of the same subject. Myogenic potential of both SCMs and mesoangioblasts showed a tendency to be decreased in the *Semitendinosus* (ST) compared to the MG muscle, rising caution to draw general conclusions and develop novel general treatments (Sibley et al., 2021) based on data from isolated muscles. The low sample size and the limited possibility to compare our results with few previously published data still need to be improved. Furthermore, unprecedented preliminary longitudinal data showed altered stem cell population proportions, as well as trends towards a reduction in SCM myogenic capacity one year after the first treatment with Botulinum Neurotoxin. Future research will be focussing on the observed stem cell phenotype, muscle composition and in combination with additional clinical data, this may lead to a further understanding of the development and complexity of CP muscle pathology.

Ethics approval and consent to participate

The studies involving human participants were reviewed and approved by the Ethical Committee of the University Hospitals of Leuven, Belgium (S61110 and S62645). Written informed consent to participate in this study was provided by the participants' legal guardian/next of kin.

Authors' contributions

All authors conceived and discussed experiments, read and approved the final version of the manuscript. In particular, EDW and AVC are pediatric orthopaedic surgeons, collecting the muscle microbiopsies and together with EH were responsible for patient recruitment. MC, JM, JD and DC performed the experiments. MC, JM, and DC analyzed the data and prepared the figures. MC wrote the manuscript. GG, MS, AVC, KD and DC edited and revised the manuscript.

Contributions to the field

Cerebral Palsy (CP) is a group of disorders that affect muscle movement and coordination and is with an incidence of 2–3 per live births one of the most common causes to childhood physical disability. Previous studies have shown alterations in the muscle development, such as decreased muscle size, increased collagen deposition and altered stem cell features. However, more detailed information on the occurrence and development of these alterations with appropriate control data is lacking. Additionally, high levels of heterogeneity in these findings further hamper the understanding of CP muscle pathology. Therefore, we aimed to further characterize the muscle stem cells, responsible for all post-natal processes, and to investigate different factors for this observed heterogeneity, such as different assessed muscle and the assessment procedures. We have highlighted alterations in the fusion potential of satellite cell-derived myoblasts as well as raised

awareness of muscle-specificity for the reported findings. By increasing our knowledge on these crucial actors in muscle alterations, we hope to gain insights in the complex CP pathology and to ultimately improve treatment for these patients.

Funding

This project was funded by an internal KU Leuven grant (C24/18/103) and by Fund Scientific Research Flanders (FWO; grant G0B4619N). MC is the recipient of a predoctoral FWO-SB fellowship (grant 1S78421N). DC was supported by internal funding of the KU Leuven Biomedical Science group: Fund for Translational Biomedical Research 2019.

Declaration of competing interest

The authors declare that the research was conducted in the absence of any commercial or financial relationships that could be construed as a potential conflict of interest.

Acknowledgements

We warmly thank all children and their families for participating in this study. We are grateful for the contribution of Prof. MD S. Nijs and E. Nijs from the Traumatology Department, Prof. G. Molenaers and Dr. H. De Houwer from the pediatric orthopaedic department and Prof. MD G. Hens from the Ear, Nose Throat department for the contribution to the recruitment of TD children, associated to the University Hospital of Leuven, Belgium, as well as all staff involved. Special thanks to J. Uyterhoeven and L. Staut, who supported the recruitment procedure. We also want to express our gratitude towards S. Vlayen and R. Ramezankhani for providing the cell lines as positive controls for the FACS analyses.

Appendix A. Supplementary data

Supplementary data to this article can be found online at https://doi.org/10.1016/j.diff.2023.06.003.

References

Akinci D'Antonoli, T., Santini, F., Deligianni, X., Garcia Alzamora, M., Rutz, E., Bieri, O., Brunner, R., Weidensteiner, C., 2021. Combination of quantitative MRI fat fraction and texture analysis to evaluate spastic muscles of children with cerebral palsy. Front. Neurol. 12, 633808 https://doi.org/10.3389/fneur.2021.633808.

Allouh, M.Z., Yablonka-Reuveni, Z., Rosser, B.W.C., 2008. Pax7 reveals a greater frequency and concentration of satellite cells at the ends of growing skeletal muscle fibers. J. Histochem. Cytochem. 56, 77–87. https://doi.org/10.1369/jhc.7A7301.2007.

Azevedo, M., Baylies, M.K., 2020. Getting into position: nuclear movement in muscle cells. Trends Cell Biol. 30, 303–316. https://doi.org/10.1016/j.tcb.2020.01.002.

Bachman, J.F., Blanc, R.S., Paris, N.D., Kallenbach, J.G., Johnston, C.J., Hernady, E., Williams, J.P., Chakkalakal, J.V., 2020. Radiation-Induced damage to prepubertal Pax7+ skeletal muscle stem cells drives lifelong deficits in myofiber size and nuclear number. iScience 23. https://doi.org/10.1016/j.isci.2020.101760.

Bergström, J., Edwards, R.H.T., 1979. Muscle-biopsy needles. Lancet. https://doi.org/10.1016/S0140-6736(79)90542-7.

Biferali, B., Proietti, D., Mozzetta, C., Madaro, L., 2019. Fibro–adipogenic progenitors cross-talk in skeletal muscle: the social network. Front. Physiol. 10 https://doi.org/10.3389/fphys.2019.01074.

Booth, C.M., Cortina-Borja, M.J., Theologis, T.N., 2001. Collagen accumulation in muscles of children with cerebral palsy and correlation with severity of spasticity. Dev. Med. Child Neurol. 43, 314–320. https://doi.org/10.1017/s0012162201000597.

Ceusters, J., Lejeune, J.P., Sandersen, C., Niesten, A., Lagneaux, L., Serteyn, D., 2017. From skeletal muscle to stem cells: an innovative and minimally-invasive process for multiple species. Sci. Rep. 7 https://doi.org/10.1038/s41598-017-00803-7.

Chal, J., Oginuma, M., Al Tanoury, Z., Gobert, B., Sumara, O., Hick, A., Bousson, F., Zidouni, Y., Mursch, C., Moncuquet, P., Tassy, O., Vincent, S., Miyanari, A., Bera, A., Garnier, J.-M., Guevara, G., Hestin, M., Kennedy, L., Hayashi, S., Drayton, B., Cherrier, T., Gayraud-Morel, B., Gussoni, E., Relaix, F., Tajbakhsh, S., Pourquié, O., 2015. Differentiation of pluripotent stem cells to muscle fiber to model Duchenne muscular dystrophy. Nat. Biotechnol. 33, 962–969. https://doi.org/10.1038/nbt.3297.

Chang, N.C., Chevalier, F.P., Rudnicki, M.A., 2016. Satellite cells in muscular dystrophy – lost in polarity. Trends Mol. Med. 22, 479–496. https://doi.org/10.1016/j.molmed.2016.04.002.

Chen, W., Datzkiw, D., Rudnicki, M.A., 2020. Satellite cells in ageing: use it or lose it. Open Biol. 10, 200048 https://doi.org/10.1098/rsob.200048.

Choi, I.Y., Lim, H., Estrellas, K., Mula, J., Cohen, T.V., Zhang, Y., Donnelly, C.J., Richard, J.-P., Kim, Y.J., Kim, H., Kazuki, Y., Oshimura, M., Li, H.L., Hotta, A., Rothstein, J., Maragakis, N., Wagner, K.R., Lee, G., 2016. Concordant but varied phenotypes among Duchenne muscular dystrophy patient-specific myoblasts derived using a human iPSC-based model. Cell Rep. 15, 2301–2312. https://doi.org/10.1016/j.celrep.2016.05.016.

Collins, B.C., Kardon, G., 2021. It takes all kinds: heterogeneity among satellite cells and fibro-adipogenic progenitors during skeletal muscle regeneration. Development 148. https://doi.org/10.1242/dev.199861.

Contreras, O., Rebolledo, D.L., Oyarzún, J.E., Olguín, H.C., Brandan, E., 2016. Connective tissue cells expressing fibro/adipogenic progenitor markers increase under chronic damage: relevance in fibroblast-myofibroblast differentiation and skeletal muscle fibrosis. Cell Tissue Res. 364, 647–660. https://doi.org/10.1007/s00441-015-2343-0.

Contreras, O., Rossi, F.M.V., Theret, M., 2021. Origins, potency, and heterogeneity of skeletal muscle fibro-adipogenic progenitors—time for new definitions. Skeletal Muscle 11, 16. https://doi.org/10.1186/s13395-021-00265-6.

Cornelison, D.D.W., 2008. Context matters: in vivo and in vitro influences on muscle satellite cell activity. J. Cell. Biochem. 105, 663–669. https://doi.org/10.1002/jcb.21892.

Corvelyn, M., De Beukelaer, N., Duelen, R., Deschrevel, J., Van Campenhout, A., Prinsen, S., Gayan-Ramirez, G., Maes, K., Weide, G., Desloovere, K., Sampaolesi, M., Costamagna, D., 2020. Muscle microbiopsy to delineate stem cell involvement in young patients: a novel approach for children with cerebral palsy. Front. Physiol. 11 https://doi.org/10.3389/fphys.2020.00945.

D'Souza, A., Bolsterlee, B., Lancaster, A., Herbert, R.D., 2020. Intramuscular fat in children with unilateral cerebral palsy. Clin. Biomech. 80, 105183 https://doi.org/10.1016/j.clinbiomech.2020.105183.

Dayanidhi, S., Dykstra, P.B., Lyubasyuk, V., McKay, B.R., Chambers, H.G., Lieber, R.L., 2015. Reduced satellite cell number in situ in muscular contractures from children with cerebral palsy. J. Orthop. Res. 33, 1039–1045. https://doi.org/10.1002/jor.22860.

De Smedt, J., van Os, E.A., Talon, I., Ghosh, S., Toprakhisar, B., Furtado Madeiro Da Costa, R., Zaunz, S., Vazquez, M.A., Boon, R., Baatsen, P., Smout, A., Verhulst, S., van Grunsven, L.A., Verfaillie, C.M., 2021. PU.1 drives specification of pluripotent stem cell-derived endothelial cells to LSEC-like cells. Cell Death Dis. 12, 84. https://doi.org/10.1038/s41419-020-03356-2.

Dellavalle, A., Maroli, G., Covarello, D., Azzoni, E., Innocenzi, A., Perani, L., Antonini, S., Sambasivan, R., Brunelli, S., Tajbakhsh, S., Cossu, G., 2011. Pericytes resident in postnatal skeletal muscle differentiate into muscle fibres and generate satellite cells. Nat. Commun. 2, 499. https://doi.org/10.1038/ncomms1508.

Díaz-Manera, J., Gallardo, E., De Luna, N., Navas, M., Soria, L., Garibaldi, M., Rojas-García, R., Tonlorenzi, R., Cossu, G., Illa, I., 2012. The increase of pericyte population in human neuromuscular disorders supports their role in muscle regeneration in vivo. J. Pathol. 228, 544–553. https://doi.org/10.1002/path.4083.

Domenighetti, A.A., Mathewson, M.A., Pichika, R., Sibley, L.A., Zhao, L., Chambers, H. G., Richard, X., Lieber, L., 2018. Loss of myogenic potential and fusion capacity of muscle stem cells isolated from contractured muscle in children with cerebral palsy. Am. J. Physiol. Cell Physiol. 315, 247–257. https://doi.org/10.1152/ajpcell.

Fernandes, S.A., Almeida, C.F., Souza, L.S., Lazar, M., Onofre-Oliveira, P., Yamamoto, G. L., Nogueira, L., Tasaki, L.Y., Cardoso, R.R., Pavanello, R.C.M., Silva, H.C.A., Ferrari, M.F.R., Bigot, A., Mouly, V., Vainzof, M., 2020. Altered in vitro muscle differentiation in X-linked myopathy with excessive autophagy. Dis. Model. Mech. 13 https://doi.org/10.1242/dmm.041244.

Handsfield, G.G., Williams, S., Khuu, S., Lichtwark, G., Stott, N.S., 2022. Muscle architecture, growth, and biological Remodelling in cerebral palsy: a narrative review. BMC Muscoskel. Disord. 23, 233. https://doi.org/10.1186/s12891-022-05110-5.

Hogarth, M.W., Defour, A., Lazarski, C., Gallardo, E., Diaz Manera, J., Partridge, T.A., Nagaraju, K., Jaiswal, J.K., 2019. Fibroadipogenic progenitors are responsible for muscle loss in limb girdle muscular dystrophy 2B. Nat. Commun. 10, 2430. https://doi.org/10.1038/s41467-019-10438-z.

Hösl, M., Böhm, H., Arampatzis, A., Döderlein, L., 2015. Effects of ankle – foot braces on medial gastrocnemius morphometrics and gait in children with cerebral palsy. J. Child. Orthop. 209–219. https://doi.org/10.1007/s11832-015-0664-x.

Howard, J.J., Graham, K., Shortland, A.P., 2022. Understanding skeletal muscle in cerebral palsy: a path to personalized medicine? Dev. Med. Child Neurol. 64, 289–295. https://doi.org/10.1111/dmcn.15018.

Howard, J.J., Herzog, W., 2021. Skeletal muscle in cerebral palsy: from belly to myofibril. Front. Neurol. 12 https://doi.org/10.3389/fneur.2021.620852.

Htwe, O., Lloyd, S., Ng, M.H., Richard, A., Rashid, A.H.A., Naicker, A.S., Ibrahim, S., 2017. Urine hydroxyproline correlates with progression of spasticity in cerebral palsy. Electron. J. Gen. Med. 15, 1–9. https://doi.org/10.29333/ejgm/81726.

Joe, A.W.B., Yi, L., Natarajan, A., Le Grand, F., So, L., Wang, J., Rudnicki, M.A., Rossi, F. M.V., 2010. Muscle injury activates resident fibro/adipogenic progenitors that facilitate myogenesis. Nat. Cell Biol. 12, 153–163. https://doi.org/10.1038/ncb2015.

Johnson, D.L., Miller, F., Subramanian, P., Modlesky, C.M., 2009. Adipose tissue infiltration of skeletal muscle in children with cerebral palsy. J. Pediatr. 154, 715–720. https://doi.org/10.1016/j.jpeds.2008.10.046.
Kim, M., Franke, V., Brandt, B., Lowenstein, E.D., Schöwel, V., Spuler, S., Akalin, A., Birchmeier, C., 2020. Single-nucleus transcriptomics reveals functional compartmentalization in syncytial skeletal muscle cells. Nat. Commun. 11, 6375. https://doi.org/10.1038/s41467-020-20064-9.
Kuang, S., Gillespie, M.A., Rudnicki, M.A., 2008. Niche regulation of muscle satellite cell self-renewal and differentiation. Cell Stem Cell 2, 22–31. https://doi.org/10.1016/j.stem.2007.12.012.
Lieber, R.L., Domenighetti, A.A., 2021. Commentary: muscle microbiopsy to delineate stem cell involvement in young patients: a novel approach for children with cerebral palsy. Front. Physiol. 12, 945. https://doi.org/10.3389/fphys.2021.642366.
Mackey, A.L., Kjaer, M., Charifi, N., Henriksson, J., Bojsen-Moller, J., Holm, L., Kadi, F., 2009. Assessment of satellite cell number and activity status in human skeletal muscle biopsies. Muscle Nerve 40, 455–465. https://doi.org/10.1002/mus.21369.
Madaro, L., Passafaro, M., Sala, D., Etxaniz, U., Lugarini, F., Proietti, D., Alfonsi, M.V., Nicoletti, C., Gatto, S., De Bardi, M., Rojas-García, R., Giordani, L., Marinelli, S., Pagliarini, V., Sette, C., Sacco, A., Puri, P.L., 2018. Denervation-activated STAT3–IL-6 signalling in fibro-adipogenic progenitors promotes myofibres atrophy and fibrosis. Nat. Cell Biol. 20, 917–927. https://doi.org/10.1038/s41556-018-0151-y.
Marbini, A., Ferrari, A., Cioni, G., Bellanova, M., Fusco, C., Gemignani, F., 2002. Immunohistochemical study of muscle biopsy in children with cerebral palsy. Brain Dev. 24, 63–66. https://doi.org/10.1016/S0387-7604(01)00394-1.
Mathewson, M.A., Lieber, R.L., 2015. Pathophysiology of muscle contractures in cerebral palsy. Phys. Med. Rehabil. Clin. N. Am. 26, 57–67. https://doi.org/10.1016/j.pmr.2014.09.005.
Modlesky, C.M., Zhang, C., 2020. Muscle size, composition, and architecture in cerebral palsy. In: Cerebral Palsy. Springer International Publishing, Cham, pp. 253–268. https://doi.org/10.1007/978-3-319-74558-9_14.
Murach, K.A., White, S.H., Wen, Y., Ho, A., Dupont-Versteegden, E.E., McCarthy, J.J., Peterson, C.A., 2017. Differential requirement for satellite cells during overload-induced muscle hypertrophy in growing versus mature mice. Skeletal Muscle 7. https://doi.org/10.1186/s13395-017-0132-z.
Novak, I., 2014. Evidence-based diagnosis, health care, and rehabilitation for children with cerebral palsy. J. Child Neurol. 29, 1141–1156. https://doi.org/10.1177/0883073814535503.
Oskoui, M., Coutinho, F., Dykeman, J., Jetté, N., Pringsheim, T., 2013. An update on the prevalence of cerebral palsy: a systematic review and meta-analysis. Dev. Med. Child Neurol. 55, 509–519. https://doi.org/10.1111/dmcn.12080.
Palisano, R., Rosenbaum, P., Walter, S., Russell, D., Wood, E., Galuppi, B., 2008. Development and reliability of a system to classify gross motor function in children with cerebral palsy. Dev. Med. Child Neurol. 39, 214–223. https://doi.org/10.1111/j.1469-8749.1997.tb07414.x.
Palisano, R.J., Rosenbaum, P., Bartlett, D., Livingston, M.H., 2008. Content validity of the expanded and revised gross motor function classification system. Dev. Med. Child Neurol. 50, 744–750. https://doi.org/10.1111/j.1469-8749.2008.03089.x.
Pingel, J., Kampmann, M.-L., Andersen, J.D., Wong, C., Døssing, S., Børsting, C., Nielsen, J.B., 2021. Gene expressions in cerebral palsy subjects reveal structural and functional changes in the gastrocnemius muscle that are closely associated with passive muscle stiffness. Cell Tissue Res. 384, 513–526. https://doi.org/10.1007/s00441-020-03399-z.
Robinson, K.G., Crowgey, E.L., Lee, S.K., Akins, R.E., 2021. Transcriptional analysis of muscle tissue and isolated satellite cells in spastic cerebral palsy. Dev. Med. Child Neurol. 63, 1213–1220. https://doi.org/10.1111/dmcn.14915.
Romero, B., Robinson, K.G., Batish, M., Akins, R.E., 2021. An emerging role for epigenetics in cerebral palsy. J. Personalized Med. 11 https://doi.org/10.3390/jpm11111187.
Saccone, V., Consalvi, S., Giordani, L., Mozzetta, C., Barozzi, I., Sandoná, M., Ryan, T., Rojas-Muñoz, A., Madaro, L., Fasanaro, P., Borsellino, G., De Bardi, M., Frigè, G., Termanini, A., Sun, X., Rossant, J., Bruneau, B.G., Mercola, M., Minucci, S., Puri, P. L., 2014. HDAC-regulated myomiRs control BAF60 variant exchange and direct the functional phenotype of fibro-adipogenic progenitors in dystrophic muscles. Genes Dev. 28, 841–857. https://doi.org/10.1101/gad.234468.113.
Sampaolesi, M., Blot, S., D'Antona, G., Granger, N., Tonlorenzi, R., Innocenzi, A., Mognol, P., Thibaud, J.-L., Galvez, B.G., Barthélémy, I., Perani, L., Mantero, S., Guttinger, M., Pansarasa, O., Rinaldi, C., Cusella De Angelis, M.G., Torrente, Y., Bordignon, C., Bottinelli, R., Cossu, G., 2006. Mesoangioblast stem cells ameliorate muscle function in dystrophic dogs. Nature 444, 574–579. https://doi.org/10.1038/nature05282.
Sätilä, H., 2020. Over 25 Years of pediatric botulinum toxin treatments: what have we learned from injection techniques, doses, dilutions, and recovery of repeated injections? Toxins (Basel) 12, 440. https://doi.org/10.3390/toxins12070440.
Shadrin, I.Y., Khodabukus, A., Bursac, N., 2016. Striated muscle function, regeneration, and repair. Cell. Mol. Life Sci. 73, 4175–4202. https://doi.org/10.1007/s00018-016-2285-z.
Sharifiaghdas, F., Taheri, M., Moghadasali, R., 2011. Isolation of human adult stem cells from muscle biopsy for future treatment of urinary incontinence. Urol. J. 8, 54–59.
Sharma, G.R., Kumar, V., Kanojia, R.K., Vaiphei, K., Kansal, R., 2019. Fast and slow myosin as markers of muscle regeneration in mangled extremities: a pilot study. Eur. J. Orthop. Surg. Traumatol. 29, 1539–1547. https://doi.org/10.1007/s00590-019-02448-w.
Sibley, L.A., Broda, N., Gross, W.R., Menezes, A.F., Embry, R.B., Swaroop, V.T., Chambers, H.G., Schipma, M.J., Lieber, R.L., Domenighetti, A.A., 2021. Differential DNA methylation and transcriptional signatures characterize impairment of muscle stem cells in pediatric human muscle contractures after brain injury. Faseb. J. 35, 1–17. https://doi.org/10.1096/fj.202100649R.
Sidney, L.E., Branch, M.J., Dunphy, S.E., Dua, H.S., Hopkinson, A., 2014. Concise review: evidence for CD34 as a common marker for diverse progenitors. Stem Cell. 32, 1380–1389. https://doi.org/10.1002/stem.1661.
Smith, L.R., Chambers, H.G., Lieber, R.L., 2013. Reduced satellite cell population may lead to contractures in children with cerebral palsy. Dev. Med. Child Neurol. 55, 264–270. https://doi.org/10.1111/dmcn.12027.
Smith, L.R., Chambers, H.G., Subramaniam, S., Lieber, R.L., 2012. Transcriptional abnormalities of hamstring muscle contractures in children with cerebral palsy. PLoS One 7. https://doi.org/10.1371/journal.pone.0040686.
Smith, L.R., Lee, K.S., Ward, S.R., Chambers, H.G., Lieber, R.L., 2011. Hamstring contractures in children with spastic cerebral palsy result from a stiffer extracellular matrix and increased in vivo sarcomere length. J. Physiol. 589, 2625–2639. https://doi.org/10.1113/jphysiol.2010.203364.
Smith, L.R., Pichika, R., Meza, R.C., Gillies, A.R., Baliki, M.N., Chambers, H.G., Lieber, R. L., 2019. Contribution of extracellular matrix components to the stiffness of skeletal muscle contractures in patients with cerebral palsy. Connect. Tissue Res. https://doi.org/10.1080/03008207.2019.1694011.
Snijders, T., Nederveen, J.P., McKay, B.R., Joanisse, S., Verdijk, L.B., van Loon, L.J.C., Parise, G., 2015. Satellite cells in human skeletal muscle plasticity. Front. Physiol. 6, 1–21. https://doi.org/10.3389/fphys.2015.00283.
Svane, C., Forman, C.R., Rasul, A., Nielsen, C.H., Nielsen, J.B., Lorentzen, J., 2021. Quantitative MRI and clinical assessment of muscle function in adults with cerebral palsy. Front. Neurol. 12, 771375 https://doi.org/10.3389/fneur.2021.771375.
Tan, C.M., Mohd Najib, N.A., Suhaimi, N.F., Halid, N.A., Cho, V.V., Abdullah, S.I., Ismail, M.Z., Khor, S.C., Jaafar, F., Makpol, S., 2021. Modulation of Ki67 and myogenic regulatory factor expression by tocotrienol-rich fraction ameliorates myogenic program of senescent human myoblasts. Arch. Med. Sci. 17, 752–763. https://doi.org/10.5114/aoms.2019.85449.
Tedesco, F.S., Moyle, L.A., Perdiguero, E., 2017. Muscle interstitial cells: a brief field guide to non-satellite cell populations in skeletal muscle. In: Methods in Molecular Biology, pp. 129–147. https://doi.org/10.1007/978-1-4939-6771-1_7. Clifton, N.J.
Tey, S.R., Robertson, S., Lynch, E., Suzuki, M., 2019. Coding cell identity of human skeletal muscle progenitor cells using cell surface markers: current status and remaining challenges for characterization and isolation. Front. Cell Dev. Biol. https://doi.org/10.3389/fcell.2019.00284.
Uezumi, A., Fukada, S., Yamamoto, N., Takeda, S., Tsuchida, K., 2010. Mesenchymal progenitors distinct from satellite cells contribute to ectopic fat cell formation in skeletal muscle. Nat. Cell Biol. 12, 143–152. https://doi.org/10.1038/ncb2014.
Von Walden, F., Gantelius, S., Liu, C., Borgström, H., Björk, L., Gremark, O., Stål, P., Nader, G.A., PontéN, E., 2018. Muscle contractures in patients with cerebral palsy and acquired brain injury are associated with extracellular matrix expansion, pro-inflammatory gene expression, and reduced rRNA synthesis. Muscle Nerve 58, 277–285. https://doi.org/10.1002/mus.26130.
Walhain, F., Desloovere, K., Declerck, M., Van Campenhout, A., Bar-On, L., 2021. Interventions and lower-limb macroscopic muscle morphology in children with spastic cerebral palsy: a scoping review. Dev. Med. Child Neurol. 63, 274–286. https://doi.org/10.1111/dmcn.14652.
Yin, H., Price, F., Rudnicki, M.A., 2013. Satellite cells and the muscle stem cell niche. Physiol. Rev. 93, 23–67. https://doi.org/10.1152/physrev.00043.2011.
Zhou, Q., Yao, Y., Ericson, S.G., 2004. The protein tyrosine Phosphatase CD45 is required for interleukin 6 signaling in U266 myeloma cells. Int. J. Hematol. 79, 63–73. https://doi.org/10.1007/BF02983536.
Zimowska, M., Kasprzycka, P., Bocian, K., Delaney, K., Jung, P., Kuchcinska, K., Kaczmarska, K., Gladysz, D., Streminska, W., Ciemerych, M.A., 2017. Inflammatory response during slow- and fast-twitch muscle regeneration. Muscle Nerve 55, 400–409. https://doi.org/10.1002/mus.25246.